MRI-guidance for motion management in external beam radiotherapy: current status and future challenges

To cite this article before publication: Chiara Paganelli *et al* 2018 *Phys. Med. Biol.* in press https://doi.org/10.1088/1361-6560/aaebcf

MRI-guidance for motion management in external beam radiotherapy: current status and future challenges

Paganelli C.[1], Whelan B.[2], Peroni M.[3], Summers P.[4], Fast M.[5], van de Lindt T.[5], McClelland J.[6], Eiben B.[6], Keall P.[2], Lomax T.[3], Riboldi M.[7] and Baroni G.[1,8]

[1]Dipartimento di Elettronica, Informazione e Bioingegneria, Politecnico di Milano, Milano, Italy
[2]ACRF Image X Institute, Sydney Medical School, University of Sydney, Sydney, Australia
[3]Proton Therapy Center, Paul Scherrer Institute, PSI Villigen, Switzerland
[4]Divisione di Radiologia, Istituto Europeo di Oncologia IRCCS, Milano, Italy
[5]Department of Radiation Oncology, Netherlands Cancer Institute, Amsterdam, The Netherlands
[6]Centre for Medical Image Computing, University College London, London, United Kingdom
[7]Department of Medical Physics, Ludwig-Maximilians-Universität München, Munich, Germany
[8]Bioengineering Unit, Centro Nazionale di Adroterapia Oncologica, Pavia, Italy

Conflict of interest
CP, BW, MP, PS, MF, TvdL, JMC, BE, TL, MR, GB have no conflict of interest
PK is a stakeholder in SeeTreat, a start-up company to commercialize intellectual property generated through NHMRC program grant APP1036075 “The Australian MRI-Linac program”.

Corresponding author:
Chiara Paganelli
Politecnico di Milano - Dipartimento di Elettronica, Informazione e Bioingegneria
v. G. Colombo, 40
20133 Milano (Italy)
contacts:
mail: chiara.paganelli@polimi.it
office: +39 02 2399 9021
website: www.cartcas.polimi.it

Abstract

High precision conformal radiotherapy requires sophisticated imaging techniques to aid in target localisation for planning and treatment, particularly when organ motion due to respiration is involved. X-ray based imaging is a well-established standard for radiotherapy treatments. Over the last few years, the ability of Magnetic Resonance Imaging (MRI) to provide radiation-free images with high resolution and superb soft-tissue contrast has highlighted the potential of this imaging modality for radiotherapy treatment planning and motion management. In addition, these advantageous properties motivated several recent developments towards combined MRI radiation therapy treatment units, enabling in-room MRI-guidance and treatment adaptation.

The aim of this review is to provide an overview of the state of the art in MRI-based image guidance for organ motion management in external beam radiotherapy. Methodological aspects of MRI for organ motion management are reviewed and their application in treatment planning, in-room guidance and adaptive radiotherapy described. Finally, a roadmap for an optimal use of MRI-guidance is highlighted and future challenges are discussed.

1. Introduction

External beam radiotherapy is a technique in the treatment of cancer as best practice care in approximately 50% of all cancer cases (Barton et al. 2014, Rosenblatt and Zubizarreta 2017). The goal of radiotherapy is to deliver a prescribed dose to oncologic targets, whilst minimizing the dose delivered to surrounding healthy tissues. It is well known that motion of both tumour and nearby organs at risk introduces geometric uncertainties into this process, leading to potential underdosage of the target region, and/or overdosage in nearby organs at risk. As such, one of the most important advances in external beam radiotherapy has been the development of techniques for imaging, planning, and treatment of targets which move as a result of respiration, such as in the lung, liver, or pancreas (Keall et al. 2006, Korreman 2012). Many technological and methodological advances were reported over the last decade, with investments in research programs, technology transfer from research to industry, and development of new generation therapy units designed to track moving targets in real-time (Riboldi, Orecchia and Baroni 2012, Kubiak 2016, Keall et al. 2006, Chang et al. 2017, Caillet, Booth and Keall 2017).

The increased confidence in tumour localization enabled by these techniques paved the way for highly conformal and dose escalated treatments, such as hypo-fractionated photon treatments and particle therapy (Schwarz, Cattaneo and Marrazzo 2017, Kubiak 2016). Strategies to compensate and account for motion such as breath-hold, gating or tumour tracking can be adopted (Kubiak 2016, Keall et al. 2006), with the support of imaging techniques to accurately guide the treatment and perform adaptive image-guided radiotherapy by means of daily monitoring of anatomo-pathological changes (Jaffray 2012, Høyer et al. 2011, Dawson and Sharpe 2006, Connell and Hellman 2009, Verellen, De Ridder and Storme 2008). To enable the targeting of the tumour under free breathing conditions, the combination of 4D imaging for treatment planning and in-room image guided strategies is beneficial in both photon (Keall et al. 2006, Caillet et al. 2017) and particle therapy (Kubiak 2016, Riboldi et al. 2012). The rapid diffusion of 4D imaging into the clinic (Simpson et al. 2009) and the clinical evidence and perspectives of image guidance (Verellen et al. 2008) indicate the relevance of such a technology.

Despite these advances, standard X-ray imaging suffers from a number of shortcomings. Above all, poor soft tissue contrast makes it difficult to distinguish the tumour from the surrounding tissues. In order to overcome this, fiducial markers may be surgically implanted, however this is a time consuming and invasive procedure. In addition, X-ray based image guidance exposes patients to additional radiation dose, which at least in some cases may be clinically significant (Bujold et al. 2012). At present, 4D Computed Tomography (4DCT) represents the standard clinical practice for organ motion management in treatment planning (Keall et al. 2006,

Chang et al. 2017): by 2009, an estimated 44% of centres were using 4D CT, indicating an increase in update of 7% per year (Simpson et al. 2009). This 4D imaging reflects anatomy at different time points during one or more samples of breathing, but the limited number of respiratory phases cannot be considered representative of each breathing cycle (intra-fraction variability) at every therapy fraction (inter-fraction variability) (Dhont et al. 2018). Therefore, it has to be supported by on-board X-ray imaging to compensate for day-to-day variations, and by tumour motion surrogates for intra-fraction motion management during treatment (Caillet et al. 2017). Among the latter, external surrogates are clinically used to reduce X-ray imaging frequency (Caillet et al. 2017), however their reliability in terms of correlation with internal anatomy is questionable (Ruan et al. 2008).

In light of these issues, Magnetic Resonance Imaging (MRI) has emerged as an ideal technique for the guidance of high precision radiation therapy, which is a topic of growing research (Figure 1). MRI provides exquisite soft tissue contrast, radiation-free imaging, high temporal resolution with fast sequences and functional imaging. These features highlight the potential of MRI to improve treatment accuracy and precision across the entire radiotherapy workflow, particularly in the presence of organ motion. For treatment planning, the superior soft-tissue contrast of MRI can decrease organ delineation uncertainties (Schmidt and Payne 2015), whilst the dose-free nature of MRI enables multiple and extended acquisitions, accounting for cycle-to-cycle breathing variations (Kauczor and Plathow 2006, Biederer et al. 2010, Jaffray 2012, Menten, Wetscherek and Fast 2017). During treatment, the new generation of in-room MRI / X-ray treatment unit systems (Ménard and van der Heide 2014, Keall, Barton and Crozier 2014, Fallone 2014, Lagendijk et al. 2014, Jaffray et al. 2014, Mutic and Dempsey 2014) allows direct imaging and both inter- and intra- fraction treatment adaptation strategies (Bainbridge et al. 2017a, Menten et al. 2017, Hunt et al. 2018). The recent clinical application of hybrid MRI and treatment unit systems (Olsen, Green and Kashani 2014, Raaymakers et al. 2017, Kashani and Olsen 2018) represents an important milestone in external beam radiotherapy, and this technology is expected to provide improved clinical outcomes and reduce toxicities as well as efficient workflows. Finally, functional MRI can enable improved treatment prediction, functionally weighted planning, and response monitoring, thereby increasing treatment personalization across the entire workflow of radiation oncology (Menten et al. 2017, Bainbridge et al. 2017b, van der Heide et al. 2012, Kauczor et al. 2006, Prestwich, Vaidyanathan and Scarsbrook 2015).

This review aims to provide a comprehensive overview of developments in MRI-guidance and its application in external beam radiotherapy for organ motion management. Current MRI techniques to quantify organ motion are described and their applications in treatment planning, in-room guidance and adaptive radiotherapy reviewed. A specific focus is posed on the clinical application of MRI in both radiotherapy planning and treatment delivery in case of moving organs. Finally, a roadmap for an optimal use of MRI-guidance and future challenges are discussed. Article searching was performed with Scopus investigating terms “MRI-guidance in radiotherapy”, “MRI motion radiotherapy”, “organ motion in radiotherapy”, “image guided radiotherapy”. We refined searches for specific issues with terms such as “time-resolved MRI”, “4DMRI”, “MRI-linac”, “in-room MRI”, “tumor tracking”, “motion modelling”, “functional MRI in radiotherapy” and combinations thereof. Only papers published in English between January 1997 and August 2018, were included. For details on MRI basics, readers are referred to (McRobbie, Moore and Graves 2017).

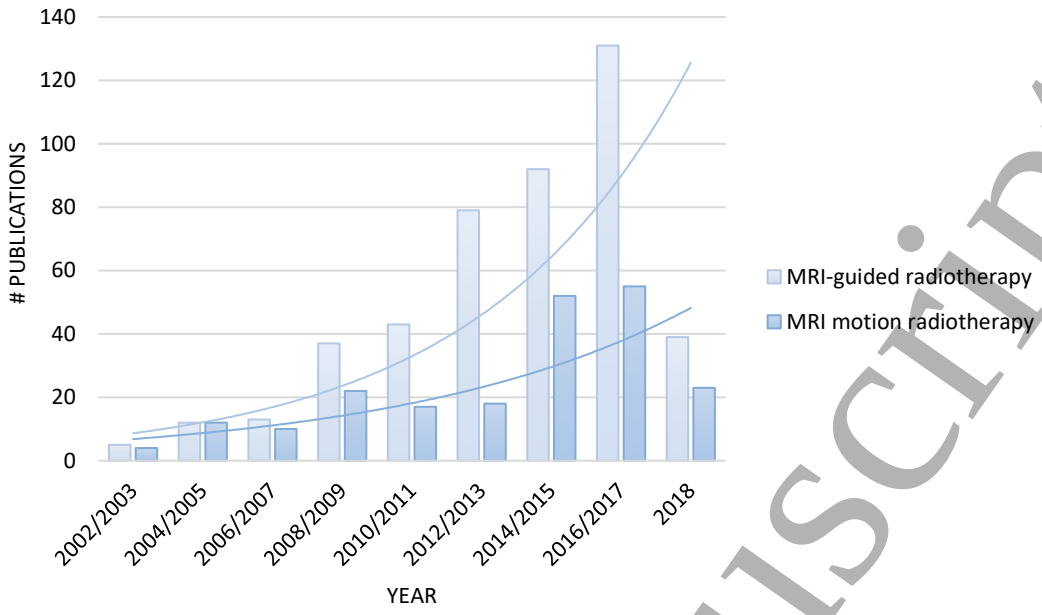

Figure 1. Trend of the publications retrieved with the search terms "MRI-guided radiotherapy", "MRI motion radiotherapy", from January 2002 to August 2018 (Scopus).

2. MRI techniques to quantify organ motion

In conventional strategies based on X-ray imaging, external surrogates represent the most widespread solution for organ motion quantification, and these have been exploited also in MRI. MR-compatible respiratory bellows (Rohlfing et al. 2004) or optical systems can be used, and combined with audio-visual biofeedback to increase breathing reproducibility (Kim et al. 2012, Lee et al. 2016). However, it is well-known that external surrogates are not always representative of the internal motion (Koch et al. 2004, Liu et al. 2004, Ruan et al. 2008). One of the main advantages of MRI is the ability to acquire the internal information over multiple respiratory cycles. At present, MRI approaches capable of resolving organ motion can be broadly classified as either time-resolved or respiratory-correlated (4D); the former delivers organ motion data in real-time at comparatively low spatial dimensionality, whilst the latter delivers comparatively high spatial dimensionality but relies on retrospective reconstruction (Figure 2). Ideally, MRI for motion quantification would involve real-time 4D MRI (i.e. sub-second 3D imaging), but due to the intrinsic trade-off between spatial and temporal resolution, this is still a challenge.

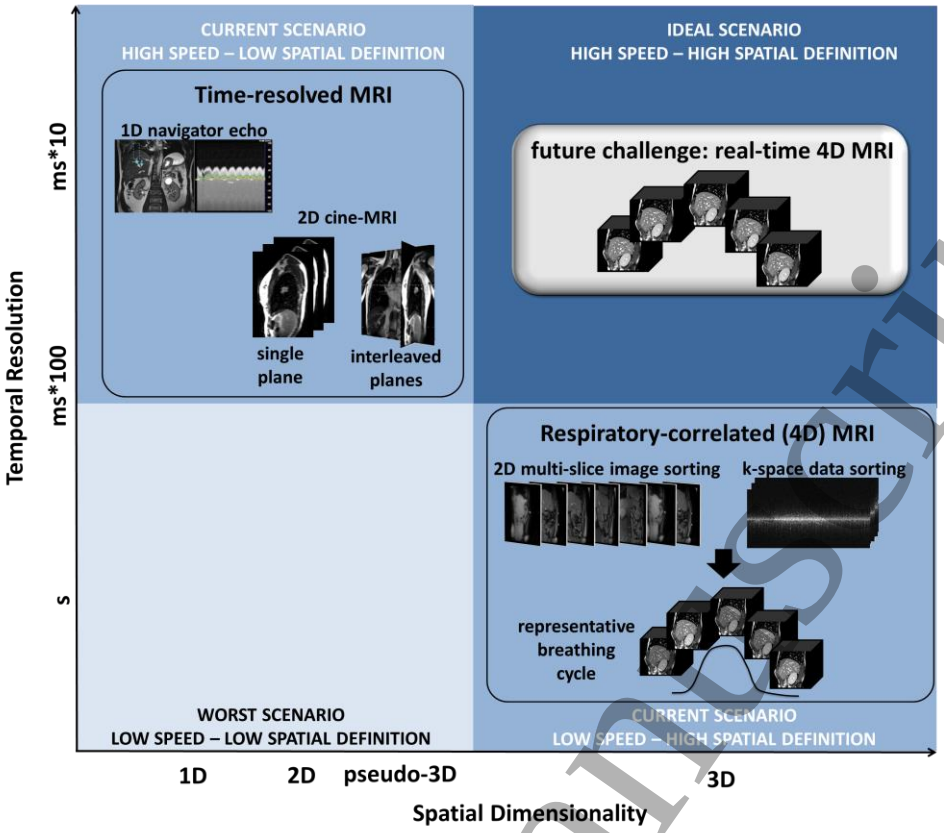

Figure 2. Image acquisition approaches in terms of temporal resolution vs. spatial dimensionality. The ideal acquisition strategy would yield real-time 4D MRI; at present this is not possible and remains a future challenge.

2.1. Time-resolved MRI

In time-resolved MRI, image acquisition is continuously performed at sub-second frame rates (Hugo and Rosu 2012). Among time-resolved solutions, the so-called navigator echo approach entails the serial acquisition of a 1D image to map the position of the diaphragm, with a temporal resolution of up to ≈10ms (Song et al. 2011). An alternative approach is fast 2D image acquisition by means of cine-MRI, which has been described in a number of studies for respiratory motion quantification, including lung, liver, pancreas and breast (Plathow et al. 2004, Rohlfing et al. 2004, Koch et al. 2004, Dowling et al. 2014, Liu et al. 2004, Blackall et al. 2006, Kauczor and Plathow 2006, Stam et al. 2013b, Kirilova et al. 2008, Bussels et al. 2003, Van Heijst et al. 2016). Balanced steady state free precession MRI (bSSFP) is a form of T2/T1-weighted gradient echo (GE) imaging sequence commonly used for cine-MRI. T2-weighted turbo spin echo (SE) sequences are an alternative to bSSFP (Kauczor et al. 2006). Specifically, (Koch et al. 2004) described the acquisition of fast dynamic 2D MR images with a temporal resolution of 450ms, whereas (Plathow et al. 2004) reported cine 2D imaging of lung cancer patients at about 300ms. Shorter acquisition times can be achieved through the use of acceleration techniques, such as parallel imaging or reduced sampling of the k-space (i.e. MRI raw data) (Heidemann et al. 2003, McRobbie et al. 2017, Pruessmann 2006) (e.g. (Griswold et al. 2002)), reaching approximately 150ms (Plathow et al. 2005, Sawant et al. 2014a). In addition, the flexibility of MRI to acquire data in arbitrary image planes allows the orientation of 2D cine-MRI along the main direction of motion (Paganelli et al. 2015b, Heerkens et al. 2014). Interleaved orthogonal planes (e.g. sagittal/coronal) represent a viable solution to provide pseudo-3D information of the tumour position near the slices intersection (Bjerre et al. 2013, Sawant et al. 2014b, Tryggestad et al. 2013b). Also for pseudo-3D acquisitions, parallel imaging techniques (Barth et al. 2016) have been exploited to allow the acquisition of simultaneous orthogonal images (Mickevicius and Paulson 2017b), thus reducing the acquisition time and improving the respiratory motion description.

2.2. Respiratory-correlated (4D) MRI

Time-resolved 2D approaches do not enable a full 3D motion description; for this time-resolved 3D images (i.e. real-time 4DMRI) would be required. However, this is currently constrained by the limited frequency at which full 3D volumes can be acquired on the current generation of scanners (acquisition time on the order of seconds). In many approaches, the limited frequency at which full 3D volumes can be acquired requires the patient to breathe slowly or limits image quality (e.g. field of view, spatial resolution) (Blackall et al. 2006, Plathow et al. 2006, Dinkel et al. 2009, Plathow et al. 2009).

To bypass this limitation, developments have entailed 2D multi-slice cine-MRI acquisitions which are sorted and stacked into a 4DMRI image, deriving one representative breathing cycle like in conventional 4DCT. In the majority of cases, retrospective sorting is applied, although in few studies prospective gating with predefined bins was also reported (Tokuda et al. 2008, Hu et al. 2013, Du et al. 2015, Li et al. 2017). In retrospective methods inherited from 4DCT, sorting of slices is usually based on an external surrogate (Hu et al. 2013). Different strategies were investigated to improve the performance of the external surrogate, either making use of audio-visual biofeedback (To et al. 2016b) or advanced sorting (Liu et al. 2015, Liang et al. 2016, Tryggestad et al. 2013d, Du et al. 2015). As previously mentioned however, the use of internal breathing surrogates directly extracted from the acquired 2D images has been shown to increase robustness in organ motion description with respect to external surrogates (Stemkens et al. 2015, Liu et al. 2016a, Li et al. 2017). Two main methods based on navigator sequences (Von Siebenthal et al. 2007, Tokuda et al. 2008, Wachinger et al. 2012) or image-derived approaches (Cai et al. 2011, Fontana et al. 2016, Paganelli et al. 2015c, Liu et al. 2014a, Hui et al. 2016, van de Lindt et al. 2018b, Liu et al. 2017, van de Lindt et al. 2018a, Uh, Khan and Hua 2016) are reported in the literature, relying on the acquisition of a navigator for sorting data, or on the derivation of the information directly from the data itself, respectively. These have been investigated with different image acquisition schemes (e.g. cine, sequential or interleaved) (Liu et al. 2015, Liu et al. 2016a) and plane orientations. Table 1 provides an overview of these methods based on prospective and retrospective image sorting. To our knowledge, a comprehensive comparison of these approaches for the evaluation of the best solution is not available, thus limiting their application in a clinical setting. Visual biofeedback was compared against a free-breathing acquisition (To et al. 2016b), whereas a direct comparison of an internal surrogate (1D navigator) with a concurrently acquired external surrogate was reported (Li et al. 2016). Multi-slice 2D acquisition based on navigator approaches can substantially reduce image artefacts compared with some of the image-derived approaches (Paganelli et al. 2018) and could describe intra-cycle variations more effectively (Von Siebenthal et al. 2007). One limitation of the navigator methods, however, is that they would require sequence modification and may result in longer acquisition time, which is instead overcome by image-based approaches exploiting slice acquisition modality without a navigator. Nevertheless, parallel imaging solutions based on the simultaneous acquisition of image data and navigator can speed up scanning time (Celicanin et al. 2015). Among the solutions reported in the literature (Table 1), the sagittal orientation has been the most wide-spread imaging direction, allowing reduced sorting artefacts and a more comprehensive respiratory motion quantification (Liu et al. 2014a). However, the trade-off between acquisition time, field of view and resolution as well as the clinical experience derived from 4DCT, make axial acquisition an alternative anatomical direction to investigate (van de Lindt et al. 2018b).

Alternative approaches that work directly in k-space rather than image domain have also been investigated. These methods sort the k-space data into respiratory bins prior to reconstructing into image space (Breuer et al. 2018, Buerger et al. 2012, Deng et al. 2016, Feng et al. 2016, Feng et al. 2014, Weick et al. 2017, Küstner et al. 2017, Weiss et al. 2017, Zucker et al. 2017, Jiang et al. 2017b, Mickevicius and Paulson 2017a, Rank et al. 2016). In order to sort the data, a breathing signal can be extracted directly from the k-space, an approach which is referred to as self-gated or self-navigated acquisition. This is achieved by frequently sampling the centre of k-space, and using this data to form a 1D breathing signal. Many of the k-space based methods use radial acquisition schemes (Buerger et al. 2012, Deng et al. 2016, Feng et al. 2016, Feng et al. 2014, Jiang et al. 2017b, Mickevicius and Paulson 2017a, Zucker et al. 2017) as these sample the centre of k-space with every

spoke, making them well suited for self-gating, but cartesian acquisition schemes have also been used (Breuer et al. 2018, Küstner et al. 2017, Weick et al. 2017).

Parallel imaging and under-sampling schemes (Pruessmann 2006, Heidemann et al. 2003, McRobbie et al. 2017, Lustig et al. 2008), can be utilised to help maximize spatial coverage, to improve spatial resolution while respecting a clinically feasible total acquisition time of a few minutes or less (Küstner et al. 2017, Mickevicius and Paulson 2017a, Feng et al. 2014). Advanced approaches that use deformable image registration to include motion correction in the reconstruction process have been proposed for reducing the acquisition time even further (37-41 s) while maintaining high quality images (Rank et al. 2017, Rank et al. 2016), but this comes at the expense of long reconstruction times. A recent comparison of several methods showed that it is possible to get good quality images with a combined acquisition and reconstruction time of less than 5 minutes (Mickevicius and Paulson 2017a). Such methods hold promise for both planning and adapting radiotherapy treatments, but currently they are still 'research methods'. In fact, these require customised sequences and reconstruction methods and are not widely available on clinical scanners, limiting their use compared to some of the image-domain based methods.

Table 1. Prospective and retrospective 4D MRI sorting methods based on multi-slice 2D image acquisitions.

	Method	Sorting	MR sequence	Slice orientation	Slice acquisition modality	Slice acquisition time [ms]
(Von Siebenthal et al. 2007)	2D navigator	Retrospective	2D bSSFP	sagittal	interleaved	≈180-190
(Tokuda et al. 2008)	1D navigator	Prospective	2D multi-slice gradient echo / spin echo	sagittal	adaptive (interleaved)	n.a.
(Cai et al. 2011)	body area	Retrospective	2D bSSFP	axial	cine	≈330
(Wachinger et al. 2012)	2D navigator + manifold learning	Retrospective	2D bSSFP	sagittal	interleaved	≈180-190
(Tryggestad et al. 2013c)	external+ average 4DMRI	Retrospective	2D bSSFP / SSFSE	sagittal / coronal	Interleaved / ascending	≈300/400
(Hu et al. 2013)	external	Prospective	2D TSE	axial / sagittal	interleaved	≈270
(Liu et al. 2014b)	body area	Retrospective	2D bSSFP	sagittal	cine	≈500/600
(Paganelli et al. 2015c)	image similarity	Retrospective	2D bSSFP	sagittal	interleaved	≈180
(Du et al. 2015)	external signal	Prospective	2D TSE	sagittal	interleaved	≈380
(Liu et al. 2015)	external signal + improved binning	Retrospective	2D SSFSE	axial	sequential	≈500
(Fontana et al. 2016)	image similarity	Retrospective	2D bSSFP	axial	interleaved	≈400
(Hui et al. 2016)	body area + Fourier-transform	Retrospective	2D bSSFP	sagittal	sequential (with manual slice adjustment)	≈160
(Liang et al. 2016)	external (probability-based)	Retrospective	2D bSSFP	axial	cine / sequential	n.a.
(Uh et al. 2016)	dimensionality reduction	Retrospective	2D bSSFP	sagittal	alternating paired slices	≈330
(To et al. 2016a)	external + visual feedback	Prospective	2D TSE	coronal	interleaved	≈400
(Li et al. 2017)	external / 1D navigator	Prospective	2D TSE	sagittal / coronal	sequential	≈500/700
(Liu et al. 2017)	sagittal/coronal diaphragm point-of-intersection	Retrospective	2D bSSFP	sagittal + coronal	cine	330
(van de Lindt et al. 2018b)	image similarity	Retrospective	2D TSE	axial	interleaved	330
(van de Lindt et al. 2018a)	image similarity	Retrospective	2D TSE/TFE	coronal	interleaved	316/366

bSSFP: balanced steady state free precession sequence (gradient echo); SSFSE: single-shot fast spin echo; TSE: turbo-spin echo; TFE: turbo-field echo. n.a.: not available.

3. MRI for organ motion management in treatment planning

In order to accurately design treatment plans in the presence of respiratory motion, accurate description of organ motion is required. In recent years, there has been substantial and growing efforts to incorporate time-resolved 2D and 4D MRI into radiotherapy treatment planning for organ motion management, either to complement CT or as the sole imaging modality (Schmidt and Payne 2015, Kashani and Olsen 2018).

3.1. MRI-guided treatment planning

Gated treatment approaches

In gated treatments, the treatment plan is designed assuming that the beam is only turned on when the tumour is in a pre-defined position, with a typical recommendation for gating windows that residual tumour motion is less than 5 mm (Keall et al. 2006). In order to perform gating, a real-time indicator of tumour position is required and be consistent between planning and treatment. In conventional X-ray imaging, surrogates are typically acquired from implanted or external fiducials, with limitations due to invasiveness as well as poor correlation with internal anatomy (Park et al. 2018, Ruan et al. 2008). With this respect, MRI enables a non-invasive and more effective method to directly visualise target structures. Cine-MRI has been used to show that surrogacy uncertainties can cause gating errors of up to 38% (Feng et al. 2009, Cai et al. 2010, Liu et al. 2004). Moreover, cine-MRI acquired at different sessions (2-week interval) was exploited for the definition of optimal gating windows (Liu et al. 2004), based on the relationship between the lung and skin movement and accounting for inter- and intra- fraction breathing variability. Finally, the use of time-resolved MRI to directly derive an internal surrogate for gating purposes was proposed, and its application on the new in-room MRI integrated systems described (Crijns et al. 2011, Mutic and Dempsey 2014) (Section 4.1). For the planning of gated treatments with cine-MRI, the Viewray system relies on the acquisition of pre-treatment breath-hold MRI acquisitions (Bohoudi et al. 2017, Acharya et al. 2016). These are used for contour propagation from CT, considering safety margins to account for free-breathing variations during treatment (see section 4.2 for additional details).

Although gating approaches are used in radiotherapy, it has to be noted that planning and treating for only one phase of the breathing cycle allows one to ‘freeze’ tumour motion at the expense of reduced treatment efficiency and increased complexity.

ITV approaches

The most widely adopted approach to deal with anatomic motion in radiotherapy is to place a treatment margin around the target volume during the treatment planning phase (Van Herk 2004). In the case of respiratory motion, the treatment volume is typically expanded to encompass the full extent of tumour motion measured during planning. Treatment is then carried out, based on the assumption that the breathing cycle determined during planning is consistent and reproducible throughout treatment. This is the so-called “Internal Target Volume” (ITV) approach (ICRU 1999). Current standard of practice is to design the ITV based on 4DCT, which sorts data to derive a patient representative breathing cycle. Since substantial cycle-to-cycle breathing variations may occur, the ITV calculated on this single cycle may differ from the ITV obtained averaging over many breaths, with potential detriment of treatment accuracy (Ge et al. 2013, Thomas et al. 2017). In this context, the use of extended cine-MRI acquisitions has been demonstrated to detect larger differences in tumour motion (up to 1cm) when compared with 4DCT, and therefore to reduce uncertainties associated with cycle-to-cycle breathing variations in the ITV, with improved margins definition (Akino et al. 2014, Fernandes et al. 2015, Cai, Read and Sheng 2008, Tryggestad et al. 2013c, Park et al. 2018). Cine-MRI was also used to generate maximum intensity projection images, which could be used to define the ITV (Adamson et al. 2010). Based on these studies, the inclusion of dynamic MRI over extended imaging periods has the potential to increase the accuracy of motion encompassing treatment approaches, by providing a more comprehensive evaluation of motion at the planning phase. However, even assuming that motion encompassing planning techniques, such as ITV, can adequately compensate for tumour motion during

treatment, they still suffer from the shortcoming that an increased amount of healthy tissue is irradiated (Ehrbar et al. 2017).

Mid-position and probabilistic approaches

In the mid-position approach, the average position (or the phase closest to the average position in case of mid-ventilation) of the tumour throughout the breathing cycle is determined, and a planning volume defined around this (Wolthaus et al. 2006, Wolthaus et al. 2008). Such an approach results in smaller target volumes, but similar dosimetric outcomes compared to the ITV approach (Lens et al. 2015). An extension to the mid-position approach is probabilistic treatment planning, in which treatment uncertainties are explicitly taken into account during the plan optimisation process (Unkelbach and Oelfke 2004, Li and Xing 2000).

As with ITV approaches, the major limitation of mid-position and probabilistic approaches is the limited amount of information on tumour motion provided by a single 4DCT scan, because the average position of the tumour may differ across different breathing cycles. It was demonstrated that cine-MRI imaging is useful for assessing the probability density function or mean tumour position on multiple breathing cycles, and that errors tend to decrease with extended imaging times, typically stabilizing after approximately three to five minutes (Cai et al. 2006, Cai et al. 2008, Tryggestad et al. 2013a). These results demonstrate the utility of dynamic MRI to enable more accurate treatment planning in mid-position and probabilistic approaches.

Acquiring mid-position images with MRI can be challenging due to the high velocity of the tumour at mid ventilation. One approach is to warp a high quality end-exhale image to the mid-ventilation using deformable image registration (van de Lindt et al. 2016). Alternatively, (Stemkens et al. 2017) proposed an approach in which a mid-position image is derived from a 4DMRI acquisition in a similar fashion as for 4DCT (Figure 3). (McClelland et al. 2017) presented a framework for fitting a motion model directly to unsorted multi-slice 2D data, so that they can be combined to form a high-quality 3D volume representing the time-averaged anatomy.

4D planning

Treatment planning is typically carried out on a static anatomical image, even though it is known that the anatomy features a dynamic behaviour. An alternative approach is 4D planning, in which anatomical motion is explicitly taken into account during dose calculation and optimization, by calculating the plan on each phase of a 4D image and accumulating the dose or directly including the time dependence of the delivery fluence together with anatomical changes (Hugo and Rosu 2012, Chang et al. 2017, Rosu and Hugo 2012).

For the case where a treatment plan is explicitly designed to be robust against motion (e.g. ITV or mid-position/ventilation), the differences between 3D and 4D dose calculations are usually minimal (Rosu and Hugo 2012). However, for advanced delivery strategies, such as multi-leaf-collimator tracking and active scanning proton therapy (Chang et al. 2017), the role of 4D planning may become more important. In these cases, 4D planning can be used to generate a motion-robust plan, providing a better estimate of the delivered dose (Bernatowicz et al. 2017, Zhang et al. 2014, Al-Ward et al. 2018).

The utility of 4DMRI in providing an extended 4D dataset for dose calculations was demonstrated in proton therapy, where organ motion can strongly affect the dose distribution (Boye, Lomax and Knopf 2013, Bernatowicz et al. 2016, Zhang et al. 2016). The method is based on using image registration to warp a static CT with the motion information provided from a 4DMRI, thus creating a combined 4DCT(MRI) dataset, which allows the cycle-by-cycle description of breathing motion. This approach allows the inclusion of respiratory organ motion into 4D dose calculations on the basis of the motion derived by the 4DMRI. A first validation of 4D dose calculation based on 4DCT(MRI) was recently provided by (Bernatowicz et al. 2016, Bernatowicz et al. 2017) for clinical liver cancer cases, in which 93% of dose calculation points were within 3%/3mm for 4D dose calculations based on 4DCT and 4DCT(MRI) (Figure 3). This approach is particularly useful to reduce the maximum dose to critical structures while maintaining target dose coverage in the presence of organ motion. However, a high sensitivity to motion variability between the optimised and tested scenario was also described, as well as the restriction of the model to the target organ (e.g. lung, liver), which may result in a sub-optimal definition of the motion extracted at the structures next to the target.

3.2. MRI-based dose calculation

The most substantial limitation to the use of MRI in treatment planning is that MRI does not provide the electron density information needed for dose calculations. As such, research efforts were aimed at trying to approximate electron density directly from MR images (so called 'pseudo-CT' or 'synthetic-CT'). Typically, dose calculation accuracy of within 2% with respect to the gold standard CT-based planning has been considered acceptable (Edmund and Nyholm 2017, Venselaar, Welleweerd and Mijnheer 2001). Various techniques exist to approximate electron density data from MRI, such as bulk-density, atlas-based or machine learning solutions (Edmund and Nyholm 2017). These were investigated in great detail for 3D MRI imaging, particularly in relatively homogenous sites such as the brain and pelvis, and MRI-based planning was successfully integrated in clinical workflows (Edmund and Nyholm 2017, Johnstone et al. 2017), with some early work also carried out for proton therapy (Maspero et al. 2017). On the other hand, synthetic-CT generation in sites affected by respiratory motion (e.g. lung, liver, breast, pancreas, kidney) has been far less investigated, with only one published paper that investigated MRI-based planning in sites affected by motion (Jonsson et al. 2010). The reasons for this are twofold. First, these sites tend to have more complex and heterogeneous electron density distributions, caused by a wider variety of tissue types (e.g. lung, bone and soft tissue). This means that errors in the synthetic-CT data are more likely to produce errors in dosimetry compared to homogeneous sites such as brain. Second, the presence of substantial respiratory motion makes the accurate generation of electron density data particularly challenging.

For ITV, mid-position/ventilation, or respiratory gating, 3D electron densities may be sufficient for planning, if 4D dose optimisation or tumour tracking is applied, electron density is desired for the full 4D dataset. A first order approach to derive a pseudo-CT, consists in the previously mentioned bulk-density assignment (Kerkhof et al. 2010), in which an automatically generated body contour is filled with Hounsfield Units equal to water, while other voxels are set to air. This approach has been investigated in abdominal sites for both static (Stam et al. 2013a) and motion-compensated planning relying on 4DMRI data (Glitzner et al. 2015a, Stemkens et al. 2017). Another solution is the previously mentioned 4DCT(MRI) approach, which uses the motion information provided by 4DMRI to warp a 3DCT dataset relative to one single respiratory phase (Boye et al. 2013).

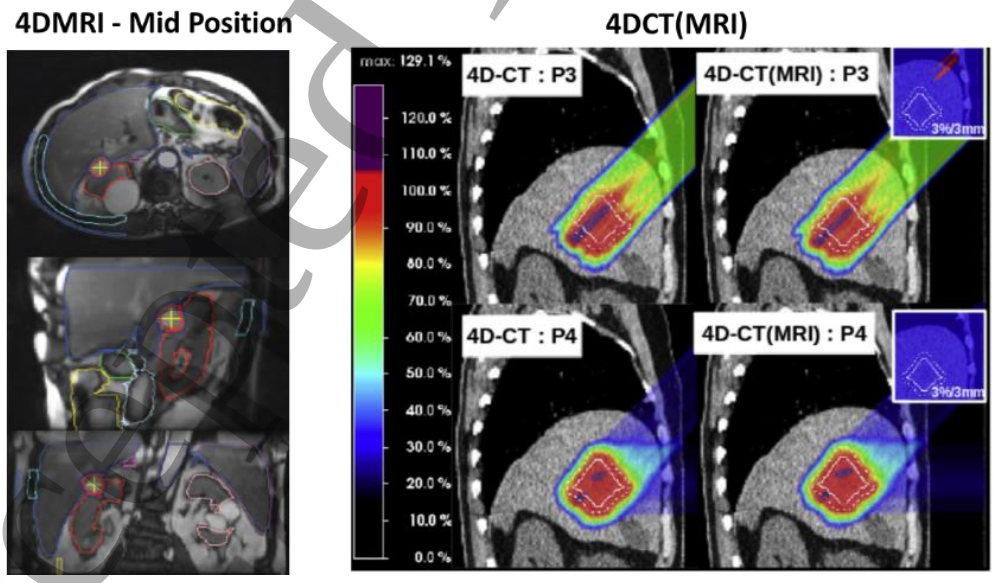

Figure 3. 4DMRI in treatment planning. 4DMRI acquisitions with contours defined on the Mid Position on the left [reprinted with permission from (Stemkens et al. 2017)]. 4DCT vs. 4DCT(MRI) approaches for proton dose calculation on the right [reprinted with permission from (Bernatowicz et al. 2016)].

4. MRI for organ motion management in treatment delivery

Besides the integration of MRI into radiotherapy treatment planning (Section 3), a substantial impact is expected from the use of MRI image guidance during treatment delivery, which is now available through a new generation of combined in-room MRI-treatment units. The use of such systems is expected to allow on-line image acquisitions just before and during treatment. This aims at quantifying inter- and intra-fraction anatomo-pathological changes by means of imaging, which could be used to accurately deliver the planned dose based on the current changing anatomy or to entirely create a new plan, thus performing adaptive treatments (Verellen et al. 2008, Hunt et al. 2018).

4.1. In-room MRI radiotherapy systems

A number of in-room MRI guidance systems are described in the literature (Jaffray et al. 2014, Fallone 2014, Keall et al. 2014, Lagendijk et al. 2014, Mutic and Dempsey 2014), two of which developed by commercial entities and treating patients: the Viewray MRIdian system and the Elekta-Unity system (Figure 4, panel A). The first treatments were carried out using the Cobalt-based Viewray MRIdian in 2014 (Olsen et al. 2014), while the world's first MRI-Linac treatment using the Elekta-Unity was in 2017 (Raaymakers et al. 2017). Both systems utilize configurations in which the treatment beam is oriented perpendicular to the magnetic field (Figure 4, panel B). In this configuration, the superior/inferior axis of patient is aligned with the magnetic field in the same manner as a conventional MRI scanner, and the linac can rotate independently of the magnet and patient. However, magnetic fields applied perpendicular to the treatment beam can substantially perturb dose deposition compared to zero field situation, particularly for the higher field Elekta-Unity system. In many situations, these effects can be compensated for using advanced treatment plan optimisation strategies (Raaijmakers et al. 2007). An alternative approach is to change the relative configuration of the radiation source and MRI scanner, such that the treatment beam and the magnetic field of the MRI scanner are parallel to each other (the 'in-line' approach, Figure 4, panel B). This approach is being developed independently by two academic groups, and can minimize or even exploit the effect of the magnetic field on the dose distribution via penumbral trimming and electron focusing effects (Oborn et al. 2016) (Alnaghy et al. 2017). However, the same physical mechanisms can also cause problems in certain scenarios, with increases in skin dose up to 1400% observed (Oborn et al. 2014). It appears that this problem can be largely mitigated either through optimisation of the magnetic fringe field or electron purging devices (Oborn et al. 2014, Keyvanloo et al. 2012). From a device perspective, the disadvantage of the in-line approach is that substantial redesign of the MRI magnet is required, and that in order to provide rotation between the beam and the patient, either the MRI scanner or the patient must be rotated, both of which are challenging (Keall et al. 2014, Whelan et al. 2017).

A solution which avoids all of these problems is the MRI-on-rails approach (Jaffray et al. 2014), in which a "near-room" MRI scanner can be moved into the treatment room for pre-treatment imaging, and removed afterwards. This approach has the advantage that the magnet can be used for multiple purposes, little redesign of existing equipment is required, and interference between the MRI scanner and radiotherapy equipment is minimized. On the other hand, the MRI cannot be used for intra-fraction monitoring, and additional time is required to move the MRI scanner in and out of the room. A similar approach using a 1.5 T scanner was developed in Umea in which the patient rather than the MRI scanner is moved (Karlsson et al. 2009, Menten et al. 2017), although this system has recently been decommissioned and replaced with a PET/MRI scanner (Brynolfsson et al. 2018). Table II shows a comparison of existing in-room/near-room MRI systems.

In addition to the existing in-room MRI systems for photon-based treatments, recent studies have started investigating the possibility of integrating MRI with particle therapy (Oborn et al. 2017, Hartman et al. 2015, Kurz et al. 2017). This concept combines the high precision of particle therapy with the high accuracy enabled by in-room MRI. However, the engineering challenges inherent to in-room photon guided system are magnified for particle systems, due to the size and complexity of these particle therapy gantries, and the use

of large scanning magnets which must be rapidly switched to steer the beam. In addition, magnetic fields distort particle beams and this must be compensated for. These issues were investigated in a recent publication by Oborn et al. (Oborn et al. 2017).

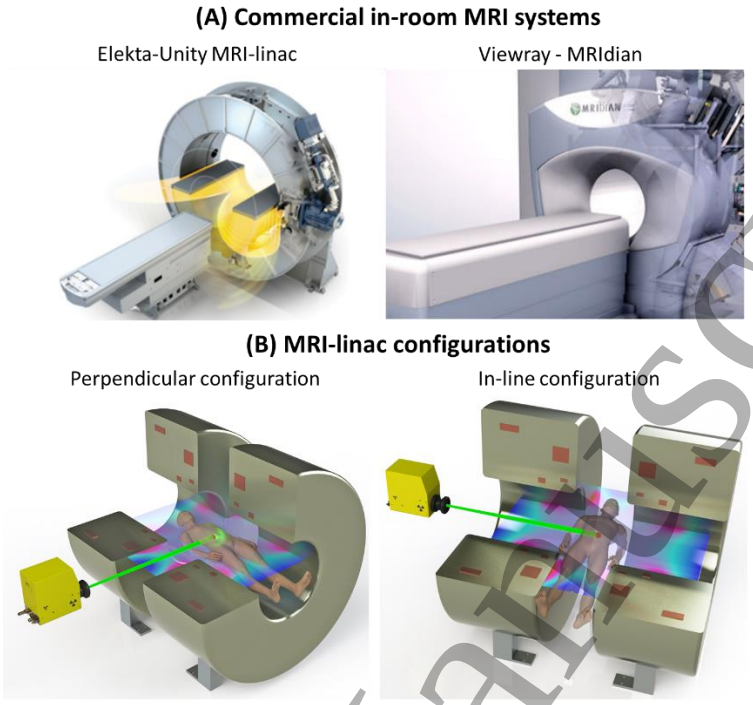

Figure 4. In-room MRI systems. (A) Commercial systems: Elekta-Unity MRI-Linac and Viewray MRIdian. (B) MRI-Linac configurations: MRI-Linac systems can be constructed in either the perpendicular configuration, or the in-line configuration (the images shown here are based on the Australian prototype system, which was designed to facilitate operation in both configurations).

Table 2. Comparison of existing in-room or near-room MRI systems.

System	X-ray source	Status	Field orientation	Field strength	Gradient strength/ slew rate
Elekta Unity	7 MV linac	Commercial system	Perpendicular	1.5 T	15 mT/m 65 T/m/s
Viewray MRIdian	Cobalt or 6 MV linac	Commercial system	Perpendicular	0.35 T	18 mT/m 200 T/m/s
Australia	6 MV linac	Research prototype	In-line/ Perpendicular	1.0 T	10 mT/m 225 T/m/s
Alberta / MagnetTx	6 MV linac	Research prototype	In-line	0.56 T	20 mT/m 66 T/m/s
Princess Margaret Hospital	Varian TrueBeam linac	One off clinical facility	n.a.	1.5 T	33 mT/m 170 T/m/s
Umea University (near-room)	Siemens Oncor linac	One off clinical facility	n.a.	1.5 T	33 mT/m 170 T/m/s

n.a.: not applicable

4.2. MRI-guided treatment delivery

Inter-fraction motion management

Inter-fraction motion management refers to the acquisition of imaging data before each treatment session to daily quantify anatomo-pathological changes for an accurate delivery of the planned dose.

In MRI-guided treatments, there have been promising results on the use of MRI for on-line inter-fraction motion quantification of pancreatic (Jiang et al. 2017a) and breast cancers (Acharya et al. 2016) using the Viewray system. In a recent application of MRI in gated treatments (Bohoudi et al. 2017), high-resolution volumetric MR images of the patient were acquired immediately prior to treatment, and deformable image registration with automatic contour propagation used to account for inter-fractional changes and subsequent plan delivery. In the first experience for pancreatic stereotactic body radiotherapy, contours were first propagated from the planning scan and then manually re-contoured within 3 cm from the PTV (Planning Target Volume), while the patient was in treatment position. For ITV treatment approaches, in-room MRI was used to demonstrate that the extent of motion can differ substantially among different treatment fractions, resulting in differences in the ITV of up to 46% (Thomas et al. 2017). The latter study highlights the potential of in-room time-resolved MRI, which allowed the authors to capture extended image data for over 20 minutes. For mid-position approaches, recent studies described the acquisition of a 4DMRI to derive on-board mid-position images with in-room MRI (Stemkens et al. 2017, Kontaxis et al. 2017).

A potential issue using current MRI-Linacs systems is that couch motion is very limited. In conventional workflows, the couch is moved to facilitate the alignment of patient and beam coordinate systems (Caillet et al. 2017). Due to the constrained geometry of MRI-Linac systems (Figure 4), non-axial couch motion is either limited or non-existent. However, it has been demonstrated that couch shifts can be replaced by a 'virtual couch shift' technique, which utilises the multi-leaf-collimator to shift the plan to the new target position (Bol, Lagendijk and Raaymakers 2013, Ruschin et al. 2017). Alternatively, the creation of a new plan directly before treatment was investigated in the Viewray (Acharya et al. 2016, Bohoudi et al. 2017) and Elekta Unity systems (Raaymakers et al. 2017) (see section 4.3 for details), without the necessity of couch shifts.

Intra-fraction motion management

A number of approaches exist both in photon and particle therapy to account for intra-fraction motion (Caillet et al. 2017, Kubiak 2016), however they typically rely on the correlation between internal markers and external surrogates, rather than directly monitoring the tumour. Time-resolved MRI overcome this limitation and as such is an ideal modality for intra-fraction motion monitoring. By exploiting combined MRI-Linac systems, time-resolved MRI will become a core intra-fraction tool for MRI-guided treatments, providing real-time anatomy monitoring and facilitating multi-leaf-collimator adaptation for an accurate delivery of the planned dose.

MRI-based intra-fraction monitoring is strongly subject to considerations of spatial and temporal trade-offs (Section 2). As such, fast 2D cine-MRI has been the most investigated technique (Heerkens et al. 2014, Paganelli et al. 2015b, Koch et al. 2004, Plathow et al. 2004), with the acquisition of interleaved orthogonal (sagittal/coronal) cine-MRI slices intersecting the target to track the 3D position of the tumour (Paganelli et al. 2015a, Bjerre et al. 2013, Brix et al. 2014, Sawant et al. 2014a, Tryggestad et al. 2013a, Stemkens et al. 2016).

In addition, intra-fraction use needs real-time automatic image processing methods to extract motion information from the high-frequency cine-MRI data. Several methods were investigated such as template matching, neural networks, particle filters, landmark extraction strategies (Figure 5) and image registration (relevant references in Table 3). (Fast et al. 2017) compared some of these methodologies in lung and showed that image-based 2D tumour motion estimation is feasible with all the investigated algorithms. However, based on their results, template matching provides the best compromise between flexibility, speed and accuracy. In a study conducted by (Glitzner et al. 2015b), the delay attributed to the multi-leaf collimator adaptation was shown to be a minor contributor to the overall feedback chain as compared to the impact of imaging components such as MRI acquisition and processing (Borman et al. 2018), which therefore require mitigation strategies to predict tumour motion (Yun et al. 2012, Seregni et al. 2016, Krauss, Nill and Oelfke 2011).

The main issue with the use of 2D cine-MRI for intra-fraction monitoring is that it is difficult to track motion in the out-of-plane direction, which can result in anatomical structures appearing and disappearing from view accordingly. A possible solution is to derive the full 3D anatomical information based on one or

two dimensional data, by using global motion modelling (McClelland et al. 2013). To build such a model, first the motion is measured off-line from 4D pre-treatment images. The model is then fitted relating the motion to the surrogate data. Finally, during treatment the model is used to estimate the full 3D motion from the measured surrogate data. Global motion models have been extensively investigated for a wide range of applications and imaging modalities (McClelland et al. 2013), including the use of MRI data to provide the motion measurements and/or the surrogate data when planning and guiding radiotherapy (Fayad et al. 2012, Stemkens et al. 2017, Stemkens et al. 2016, Harris et al. 2016, McClelland et al. 2017).

However, motion models have not yet entered widespread clinical use, due to two main problems. Firstly, the relationship between the motion and surrogate data can deteriorate over time due to changes in the breathing pattern and anatomy. Secondly, the images used to measure the motion are usually respiratory-correlated, and hence do not provide a good representation of the true motion including the intra-cycle variation, and its relationship to the surrogate data (McClelland et al. 2017, Harris et al. 2016). The use of in-room MRI systems may help alleviate the first problem, as the models can be built and updated just prior to, and even during treatment delivery. The second problem can be partly addressed by the use of 4DMRI methods that try to image the intra-cycle variation (Bernatowicz et al. 2016). Alternatively, methods have been proposed that can fit the motion model directly to all the unsorted image data simultaneously (McClelland et al. 2017, Odille et al. 2008).

Table 3. Methods for tumour tracking based on cine-MRI acquisitions.

Method	Authors	Site	Field strength [T]	MR sequence	Slice orientation	Image acquisition time [ms]	Image resolution [mm]	Method accuracy [mm]	Processing time
Template matching	(Koch et al. 2004)	Lung	1.5	Fast GE	sagittal / coronal	450	n.p.	1-2	n.a.
	(Cervino, Du and Jiang 2011)	Lung	3	n.a.	sagittal	250	1.37×1.37×10	0.6	84 ms
	(Tryggestad et al. 2013a)	Lung	1.5	bSSFP	sagittal / coronal	250	2×2×5	0.7-1.6	n.a.
	(Bjerre et al. 2013)	Kidney	1.5	bSSFP	sagittal / coronal	252	1.05×1.05×7	1.15	153 ms
	(Brix et al. 2014)	Liver	1.5	bSSFP	axial / sagittal / coronal	184	1.56×1.56×1.6	1.6	90 ms
	(Shi et al. 2014)	Lung	1.5	bSSFP	sagittal	250	1.95×1.95×(12-16)	1.95	10-15 s
	(Fast et al. 2017)	Lung	1.5	bSSFP, spoiled GE	sagittal / coronal	500	1.5×1.5×3.0	1.7	1ms
Neural networks, particle filters	(Cervino et al. 2011)	Lung	3	n.p.	sagittal	250	1.37×1.37×10	1.5	150 ms
	(Gou et al. 2014)	Liver, Pancreas, stomach	1.5	bSSFP	coronal	200	1.87×1.87×7	0.70-0.92 (DSC)	1.8-33 s
	(Yun et al. 2015)	Lung	0.5	bSSFP	sagittal	280	3.1×3.1×20	0.5-0.9	40ms
	(Lee et al. 2016)	Lung	1.5	bSSFP	sagittal / coronal	303	1.48×1.48×5	n.a.	n.a.
	(Bourque et al. 2016)	Lung	1.5	bSSFP	sagittal	250	1.0×1.0×10.0	0.6-2	0.8-2
	(Fast et al. 2017)	Lung	1.5	bSSFP, spoiled GE	sagittal / coronal	500	1.5×1.5×3	2	25ms
Internal landmarks	(Paganelli et al. 2015b)	Liver	1.5	bSSFP	sagittal (oblique)	310	1.28×1.28×10	1.87	≈15min

	(Paganelli et al. 2015a)	Lung	1.5	bSSFP	sagittal / coronal	303	1.48×1.48×5	1.87	≈15min
	(Mazur et al. 2016)	Lung	0.35	bSSFP	sagittal	250	3.5×3.5×7	1.4	≈250ms
	(Fast et al. 2017)	Lung	1.5	bSSFP, spoiled GE	sagittal / coronal	500	1.5×1.5×3	2	150ms
Image Registration	(Sawant et al. 2014a)	Lung	1.5	bSSFP	sagittal / coronal	152-273	2×3×5	n.a.	n.a.
	(Heerkens et al. 2014)	Pancreas	1.5	SSFP	sagittal / coronal	500	1.4×1.4×5	n.a.	n.a.
	(Zachiu et al. 2015)	Kidney, liver	1.5	Single shot GE	coronal	83	2.5×2.5×7	≈2.5	≈25ms
	(Seregni et al. 2017)	Liver	1.5	bSSFP	sagittal (oblique)	310	1.28×1.28×10	1.28	50ms
	(Fast et al. 2017)	Lung	1.5	bSSFP, spoiled GE	sagittal / coronal	500	1.5×1.5×3	1.7	500ms

n.a.: not available
bSSFP = balanced Steady-State Free procession; SPGR = = Spoiled Gradient Echo; EPI = Echo Planar Imaging

4.3. Dosimetric evaluation and adaptation

Many of the strategies outlined above are focused on geometric motion quantification by means of image acquisition to ensure target coverage and accurately deliver the planned dose. However, an adaptive treatment strategy should also adapt treatments in response to dose. Such a workflow is termed 'closed-loop' adaptive radiotherapy, in which the adaptive decision is made on the basis of optimal dose versus dose delivered and the plan re-optimised (de la Zerda, Armbruster and Xing 2007). As for the geometrical scenario, dose adaptation can be carried out both inter- and intra- fractionally.

Whilst the potential of inter-fraction adaptation has been deeply discussed in the literature, it is only with the advent of in-room MRI guidance that this became a vendor supported on-line clinical reality. Inter-fraction dose adaptation is in fact implemented on the Viewray system (Acharya et al. 2016, Bohoudi et al. 2017), where deformable registration is used to propagate contours and Hounsfield units from the planning data, and dose calculation is performed and compared to the planned dose. A manual review triggers a decision on whether plan re-optimisation should be performed. A recent prospective trial reported promising results of this adaptive protocol in PTV dose escalation and/or simultaneous organs at risk sparing for the treatment of oligometastatic or unresectable primary malignancies of the abdomen (Henke et al. 2018). An alternative workflow was demonstrated in a trial setting using the Elekta Unity system (Raaymakers et al. 2017), in which plan re-optimisation was carried out automatically. Both workflows utilise fast Monte-Carlo based dose engines to minimise the time for re-planning. For the Viewray system, new plans can be generated in approximately 12 minutes, including manual review and re-contouring (Bohoudi et al. 2017). Plan generation using the Elekta-Unity system was reported to take approximately 5 minutes in a clinical setting (Raaymakers et al. 2017), whilst in the research setting, plan generation ranged from seconds to minutes (Bol et al. 2012). In addition, pre-beam re-planning supported by fully automatic contours propagation could save time (Kontaxis et al. 2017).

On the other hand, intra-fraction dose adaptation has yet to be clinically demonstrated but remains a tantalising prospect. An intriguing approach to this problem was recently proposed by (Kontaxis et al. 2015b), in which authors updated the treatment plan in response to the changing patient anatomy. This algorithm fundamentally differs from conventional approaches, which seek an 'optimal' solution before treatment is started. Instead, if the first delivered beamlet is sub-optimal, this is corrected via modulation of later applied beamlets, with the algorithm converging towards the ideal dose at the same time as the dose is being delivered. This approach can compensate for both inter and intra-fraction variation, as was clearly described and

demonstrated by (Kontaxis et al. 2015a). However, uncertainties in deformable image registration algorithms, as well as the computational time required by the algorithm, still represent a limitation to clinical application.

As previously discussed (Section 3.2), a major challenge for inter- and intra-fraction MRI-based dosimetric adaptation is that MRI images do not provide the electron density data needed for dose calculation. To date, the most commonly proposed approach to derive in-room electron density maps for moving targets is to propagate existing electron density information to daily MR images by using deformable image registration (Bohoudi et al. 2017, Raaymakers et al. 2017) or bulk density overrides (Glitzner et al. 2015a, Stemkens et al. 2017). Alternatives include using a 4DCT(MRI) approach (Boye et al. 2013, Marx et al. 2014) or the use of global motion models (Stemkens et al. 2017) (Figure 5). Although neither of these methods are currently implemented in real-time, they could be applied retrospectively to enable intra-fraction dose reconstruction and accumulation (Bernatowicz et al. 2016, Stemkens et al. 2017).

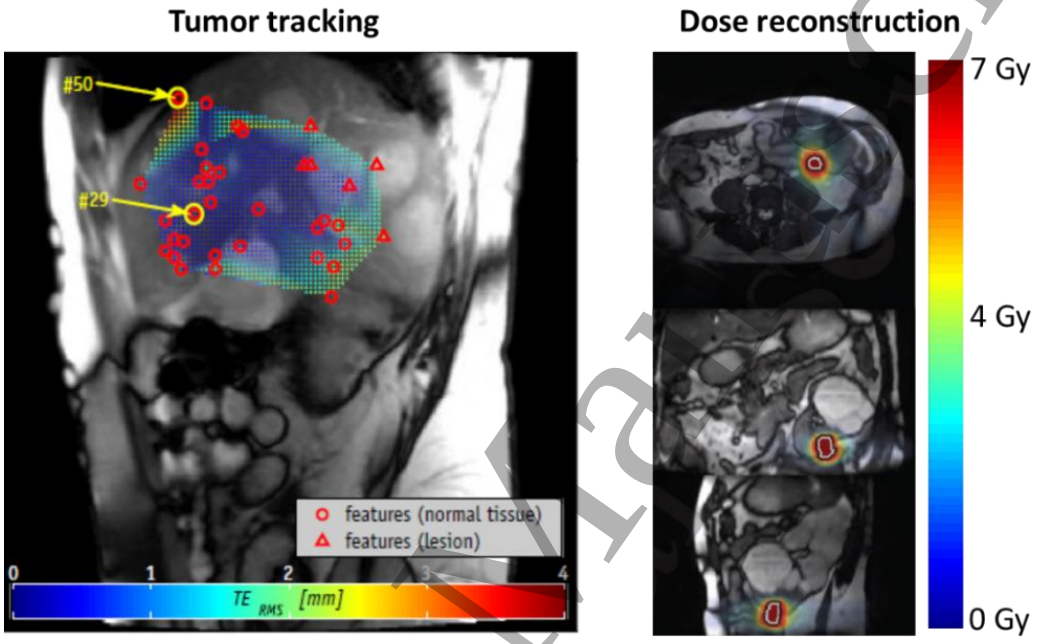

Figure 5. Time-resolved MRI in treatment delivery. An example of tumour tracking approach by means of anatomical landmarks on the left [reprinted with permission from (Paganelli et al. 2015b)]. Dose reconstruction by means of a global motion model strategy [reprinted with permission from (Stemkens et al. 2017)].

5. Conclusions and future directions

5.1. Roadmap for MRI-guidance in moving organs

MRI offers exquisite soft tissue contrast, unparalleled acquisition flexibility, dose-free imaging and functional acquisition. Due to these advantages, there is rapidly growing interest in the role of MRI in radiotherapy and in its use for organ motion management. This has motivated institutional, commercial and research efforts towards the implementation of advanced strategies to accomplish motion management. Based on the reported findings, we provide here a roadmap for an optimal use of MRI-guidance in radiotherapy, covering both treatment planning and delivery. This aims at supporting further research and potential clinical applications in the near-term. Specifically, from the literature analysis we can derive that:

- In treatment planning, both time-resolved 2D images and 4DMRI should be exploited to account for inter- and intra-fraction breathing variabilities. This will allow improved definition of personalized margin recipes and could be included in gating as well as ITV or mid-position approaches. Respiratory-correlated 4DMRI can further provide a dataset for robust planning and complement 4DCT. As reported in (Chang et al. 2017), 4D imaging should be exploited to enable 4D optimization which can improve plan robustness to intra-fractional motion for particle treatments or multi-leaf collimator tracking strategies. Vendors are therefore

encouraged to implement motion analysis tools, dynamic dose calculation and 4D robust optimization within treatment planning systems. Due to the lack of MRI-based dose planning and calculation strategies in moving organs, the 4DCT(MRI) approach represents an attractive strategy to preserve electron density information. In this case, respiratory phase correspondence and/or image registration algorithms between CT and MRI need to be validated, to provide an accurate motion description. MRI (and/or 4DMRI) can be also exploited to perform multiple/frequent acquisitions to determine whether adaptive re-planning is needed to maintain plan robustness. This is especially the case for particle centres or institutions in which in-room MRI systems are not available.

- In treatment delivery with in-room MRI systems, pre-beam/on-board images are acquired before beam on, to update the plan or to create a new one. In this case, fast treatment planning and adaptation is performed as done by the MRIdian (Viewray) and Elekta Unity treatment devices. On-line verification and quality assurance strategies for such adaptations are essential in the development of these approaches. An independent dose calculation engine could be used for verification, and retrospective dose reconstruction performed off-line.

During delivery, orthogonal sagittal/coronal cine-MR images should be acquired to allow the 3D motion estimation at the centre of the tumour. Alternatively, the sagittal direction is the favoured orientation in the literature to capture the major motion directions, and/or patient-specific evaluation based on treatment planning data could be investigated to determine the optimal cine-MRI orientation. In combination with cine-MRI acquisition, real-time tumour localization methods are likely to be implemented and integrated in the treatment workflow. These methods are essential for residual motion quantification in the gating window and for tumour tracking and multi-leaf collimator adaptation. Template matching has been shown in the literature to be an attractive solution since it is simple, robust and fast to test. However in case of tumour tracking treatments, improvements of this approach should be considered to account for non-rigid displacements as well as effects of out-of-plane motion. These could be supported by pre-beam/on-board 4DMRI and retrospective evaluations such as motion models. Additionally, prediction algorithms need to be considered when system latencies hinder acquiring information in real-time. Another important aspect to take into consideration for in-room MRI systems is the request for on-line dose evaluation and adaptation, which should be supported by vendors and integrated in the treatment workflow. Bulk density analysis could be performed as preliminary approach for on-line verification of planned dose vs. delivered dose, since in online adaptive scenarios it may be acceptable to have a lower threshold for dose calculation accuracy than for planning. Off-line verification should also be performed in this case, for example by utilising global motion models for dose accumulation.

5.2. Future challenges

Despite the potential of MRI in radiotherapy, there are a number of challenges to increasing its clinical penetration. To overcome these, technological and methodological improvements are required.

The first issue for organ motion management with MRI is the inherent trade-off between spatial and temporal resolution. The ultimate goal of ‘real-time’ 4D imaging (approximately four or more 3D volumes per second with appropriate spatial resolution) remains some distance in the future. At present, state-of-the-art imaging for motion compensation relies on time-resolved 2D cine-MRI data, which can deliver approximately four interleaved images per second. As far as 4D imaging is concerned, several approaches have been proposed relying on retrospective sorting of images or k-space data as well as motion modelling. However, further research is needed to define standards for the clinical inclusion of 4DMRI in the radiotherapy workflow.

MRI does not provide the electron density information needed for treatment planning and/or dose delivery verification. This must be overcome for fully MRI-guided treatment. For static anatomical sites such as pelvis and brain, electron density recovery from MRI images has been investigated quite extensively within the literature, and commercial products have recently been released. However, for anatomical sites where substantial motion occurs, further research is required to ensure accurate MRI-based dose calculation. Moreover, it is also important to note that MRI suffers from geometrical distortion which could affect MRI-based dose calculation and organ motion quantification. This aspect was reviewed in (Schmidt and Payne

2015) and, to our knowledge, just one publication has been reported dealing with moving organs (Torfeh et al. 2018). Effects of geometrical distortion are outside the scope of this review but require additional evaluation on the accuracy of MRI for treatment guidance and protocols should be defined to account for these uncertainties.

An additional advantage of MRI with respect to X-ray imaging is the possibility to derive functional information, which has the potential to enable increased treatment personalization across the entire radiotherapy workflow (Bainbridge et al. 2017a, van der Heide et al. 2012, Prestwich et al. 2015). However, most of functional MRI techniques in regions affected by motion under free-breathing are still in a very preliminary stage. Perfusion MRI and diffusion MRI have been investigated with in-room MRI systems to enhance tumour visibility (Wojcieszynski et al. 2016) or preliminary assess tumour response (Yang et al. 2016), but few studies dealt with organ motion management (Liu et al. 2016b). Functionally guided planning in the lung based on hyperpolarised MRI showed potentials in reducing the amount of healthy tissue irradiated and has been used to prospectively treat patients in the experimental arm of the double-blind randomised Functional Lung Avoidance for Individualized Radiotherapy (FLAIR) trial (Hoover et al. 2014). Additionally, the potential of PET/MRI has been demonstrated in both treatment planning (Brynolfsson et al. 2018) and tumour response assessment (Varoquaux et al. 2015, Daniel et al. 2017), with attainable results in providing anatomical and functional 4D maps (Fayad et al. 2017). However, further research is required in sites affected by organ motion and replication and standardization are needed before these techniques achieve the level of clinical confidence required in a treatment workflow.

In conclusion, guidelines and quality assurance strategies for clinical applications of MRI in organ motion management need to be defined to support the move of radiotherapy towards high precision techniques and personalised treatment. The growing experience in the use of MRI-Linacs is expected to contribute significantly towards this goal, especially with the support of clinical studies to evaluate the clinical impact of MRI-guided radiotherapy in sites affected by organ motion.

Acknowledgments

The authors would like to thank Dr. Teo Stanescu (Princess Margaret Cancer Centre, Toronto, Canada), Dr. Gino Fallone (University of Alberta, Edmonton, Canada) and Dr. Tufve Nyholm (Umea University, Umea, Sweden) for providing information on the Princess Margaret, Alberta/MagnetTx in-room MRI systems and Umea system, respectively. MF and TvdL would like to acknowledge that The Netherlands Cancer Institute is part of the Elekta Atlantic MR-Linac research consortium. JMC and BE are funded by the Stand Up to Cancer campaign for Cancer Research UK (C33589/CRC521) and Network Accelerator Award Grant (A219932). In addition, we would also like to acknowledge the important contributions of the anonymous reviewers.

References

Acharya, S., B. W. Fischer-Valuck, R. Kashani, P. Parikh, D. Yang, T. Zhao, O. Green, O. Wooten, H. H. Li & Y. Hu (2016) Online magnetic resonance image guided adaptive radiation therapy: first clinical applications. *International Journal of Radiation Oncology* Biology* Physics,* 94**,** 394-403.

Adamson, J., Z. Chang, Z. Wang, F. F. Yin & J. Cai (2010) Maximum intensity projection (MIP) imaging using slice-stacking MRI. *Medical physics,* 37**,** 5914-5920.

Akino, Y., R. J. Oh, N. Masai, H. Shiomi & T. Inoue (2014) Evaluation of potential internal target volume of liver tumors using cine-MRI. *Medical physics,* 41**,** 111704.

Al-Ward, S. M., A. Kim, C. McCann, M. Ruschin, P. Cheung, A. Sahgal & B. M. Keller (2018) The development of a 4D treatment planning methodology to simulate the tracking of central lung tumors in an MRI-linac. *Journal of applied clinical medical physics,* 19**,** 145-155.

Alnaghy, S. J., J. Begg, T. Causer, T. Alharthi, L. Glaubes, B. Dong, A. George, L. Holloway & P. Metcalfe (2017) Penumbral Width Trimming in Solid Lung Dose Profiles for 0.9 T and 1.5 T MRI-Linac Prototypes. *Medical Physics,* 45**,** 479–487.

Bainbridge, H., A. Salem, R. H. Tijssen, M. Dubec, A. Wetscherek, C. Van Es, J. Belderbos, C. Faivre-Finn, F. McDonald & i. A. M.-L. Consortium (2017a) Magnetic resonance imaging in precision radiation therapy for lung cancer. *Translational Lung Cancer Research,* 6**,** 689-707.

Bainbridge, H. E., M. J. Menten, M. F. Fast, S. Nill, U. Oelfke & F. McDonald (2017b) Treating locally advanced lung cancer with a 1.5 T MR-Linac–Effects of the magnetic field and irradiation geometry on conventionally fractionated and isotoxic dose-escalated radiotherapy. *Radiotherapy and Oncology*.

Barth, M., F. Breuer, P. J. Koopmans, D. G. Norris & B. A. Poser (2016) Simultaneous multislice (SMS) imaging techniques. *Magnetic resonance in medicine,* 75**,** 63-81.

Barton, M. B., S. Jacob, J. Shafiq, K. Wong, S. R. Thompson, T. P. Hanna & G. P. Delaney (2014) Estimating the demand for radiotherapy from the evidence: a review of changes from 2003 to 2012. *Radiotherapy and oncology,* 112**,** 140-144.

Bernatowicz, K., M. Peroni, R. Perrin, D. C. Weber & A. Lomax (2016) Four-dimensional dose reconstruction for scanned proton therapy using liver 4DCT-MRI. *International Journal of Radiation Oncology* Biology* Physics,* 95**,** 216-223.

Bernatowicz, K., Y. Zhang, R. Perrin, D. C. Weber & A. J. Lomax (2017) Advanced treatment planning using direct 4D optimisation for pencil-beam scanned particle therapy. *Physics in Medicine & Biology,* 62**,** 6595.

Biederer, J., C. Hintze, M. Fabel & J. Dinkel (2010) Magnetic resonance imaging and computed tomography of respiratory mechanics. *Journal of Magnetic Resonance Imaging,* 32**,** 1388-1397.

Bjerre, T., S. Crijns, P. M. af Rosenschöld, M. Aznar, L. Specht, R. Larsen & P. Keall (2013) Three-dimensional MRI-linac intra-fraction guidance using multiple orthogonal cine-MRI planes. *Physics in medicine and biology,* 58**,** 4943.

Blackall, J., S. Ahmad, M. Miquel, J. McClelland, D. Landau & D. Hawkes (2006) MRI-based measurements of respiratory motion variability and assessment of imaging strategies for radiotherapy planning. *Physics in medicine and biology,* 51**,** 4147.

Bohoudi, O., A. Bruynzeel, S. Senan, J. Cuijpers, B. Slotman, F. Lagerwaard & M. Palacios (2017) Fast and robust online adaptive planning in stereotactic MR-guided adaptive radiation therapy (SMART) for pancreatic cancer. *Radiotherapy and Oncology,* 125**,** 439-444.

Bol, G., S. Hissoiny, J. Lagendijk & B. Raaymakers (2012) Fast online Monte Carlo-based IMRT planning for the MRI linear accelerator. *Physics in medicine and biology,* 57**,** 1375.

Bol, G., J. Lagendijk & B. Raaymakers (2013) Virtual couch shift (VCS): accounting for patient translation and rotation by online IMRT re-optimization. *Physics in medicine and biology,* 58**,** 2989.

Borman, P., R. Tijssen, C. Bos, C. Moonen, B. Raaymakers & M. Glitzner (2018) Characterization of imaging latency for real-time MRI-guided radiotherapy. *Physics in Medicine & Biology,* 63**,** 155023.

Bourque, A. E., S. Bedwani, É. Filion & J. F. Carrier (2016) A particle filter based autocontouring algorithm for lung tumor tracking using dynamic magnetic resonance imaging. *Medical physics,* 43**,** 5161-5169.

Boye, D., T. Lomax & A. Knopf (2013) Mapping motion from 4D-MRI to 3D-CT for use in 4D dose calculations: A technical feasibility study. *Medical physics,* 40.

Breuer, K., C. B. Meyer, F. A. Breuer, A. Richter, F. Exner, A. M. Weng, S. Ströhle, B. Polat, P. M. Jakob & O. A. Sauer (2018) Stable and efficient retrospective 4D-MRI using non-uniformly distributed quasi-random numbers. *Physics in Medicine & Biology,* 63**,** 075002.

Brix, L., S. Ringgaard, T. S. Sørensen & P. R. Poulsen (2014) Three-dimensional liver motion tracking using real-time two-dimensional MRI. *Medical physics,* 41.

Brynolfsson, P., J. Axelsson, A. Holmberg, J. H. Jonsson, D. Goldhaber, Y. Jian, F. Illerstam, M. Engström, B. Zackrisson & T. Nyholm (2018) Adapting a GE SIGNA PET/MR scanner for radiotherapy. *Medical physics*.

Buerger, C., R. E. Clough, A. P. King, T. Schaeffter & C. Prieto (2012) Nonrigid motion modeling of the liver from 3-D undersampled self-gated golden-radial phase encoded MRI. *IEEE transactions on medical imaging,* 31**,** 805-815.

Bujold, A., T. Craig, D. Jaffray & L. A. Dawson. 2012. Image-guided radiotherapy: has it influenced patient outcomes? In *Seminars in radiation oncology*, 50-61. Elsevier.

Bussels, B., L. Goethals, M. Feron, D. Bielen, S. Dymarkowski, P. Suetens & K. Haustermans (2003) Respiration-induced movement of the upper abdominal organs: a pitfall for the three-dimensional conformal radiation treatment of pancreatic cancer. *Radiotherapy and Oncology,* 68**,** 69-74.

Cai, J., Z. Chang, Z. Wang, W. Paul Segars & F. F. Yin (2011) Four-dimensional magnetic resonance imaging (4D-MRI) using image-based respiratory surrogate: A feasibility study. *Medical physics,* 38**,** 6384-6394.

Cai, J., R. McLawhorn, P. W. Read, J. M. Larner, F. f. Yin, S. H. Benedict & K. Sheng (2010) Effects of breathing variation on gating window internal target volume in respiratory gated radiation therapy. *Medical physics,* 37**,** 3927-3934.

Cai, J., P. W. Read, T. A. Altes, J. A. Molloy, J. R. Brookeman & K. Sheng (2006) Evaluation of the reproducibility of lung motion probability distribution function (PDF) using dynamic MRI. *Physics in medicine and biology,* 52**,** 365.

Cai, J., P. W. Read & K. Sheng (2008) The effect of respiratory motion variability and tumor size on the accuracy of average intensity projection from four-dimensional computed tomography: An investigation based on dynamic MRI. *Medical physics,* 35**,** 4974-4981.

Caillet, V., J. T. Booth & P. Keall (2017) IGRT and motion management during lung SBRT delivery. *Physica Medica,* 44**,** 113-122.

Celicanin, Z., O. Bieri, F. Preiswerk, P. Cattin, K. Scheffler & F. Santini (2015) Simultaneous acquisition of image and navigator slices using CAIPIRINHA for 4D MRI. *Magnetic resonance in medicine,* 73**,** 669-676.

Cervino, L. I., J. Du & S. B. Jiang (2011) MRI-guided tumor tracking in lung cancer radiotherapy. *Physics in medicine and biology,* 56**,** 3773.

Chang, J. Y., X. Zhang, A. Knopf, H. Li, S. Mori, L. Dong, H.-M. Lu, W. Liu, S. N. Badiyan & S. Both (2017) Consensus guidelines for implementing pencil beam scanning proton therapy for thoracic malignancies on behalf of PTCOG thoracic and lymphoma subcommittee. *International Journal of Radiation Oncology* Biology* Physics,* 99**,** 41-50.

Connell, P. P. & S. Hellman (2009) Advances in radiotherapy and implications for the next century: a historical perspective. *Cancer research,* 69**,** 383-392.

Crijns, S., J. Kok, J. Lagendijk & B. Raaymakers (2011) Towards MRI-guided linear accelerator control: gating on an MRI accelerator. *Physics in medicine and biology,* 56**,** 4815.

Daniel, M., P. Andrzejewski, A. Sturdza, K. Majercakova, P. Baltzer, K. Pinker, W. Wadsak, M. Mitterhauser, R. Pötter & P. Georg (2017) Impact of hybrid PET/MR technology on multiparametric imaging and treatment response assessment of cervix cancer. *Radiotherapy and Oncology,* 125**,** 420-425.

Dawson, L. A. & M. B. Sharpe (2006) Image-guided radiotherapy: rationale, benefits, and limitations. *The lancet oncology,* 7**,** 848-858.

de la Zerda, A., B. Armbruster & L. Xing (2007) Formulating adaptive radiation therapy (ART) treatment planning into a closed-loop control framework. *Physics in medicine and biology,* 52**,** 4137.

Deng, Z., J. Pang, W. Yang, Y. Yue, B. Sharif, R. Tuli, D. Li, B. Fraass & Z. Fan (2016) 4D MRI using 3D radial sampling with respiratory self-gating to characterize temporal phase-resolved respiratory motion in the abdomen. *Magnetic resonance in medicine,* 75**,** 1574.

Dhont, J., J. Vandemeulebroucke, M. Burghelea, K. Poels, T. Depuydt, R. Van Den Begin, C. Jaudet, C. Collen, B. Engels & T. Reynders (2018) The long-and short-term variability of breathing induced tumor motion in lung and liver over the course of a radiotherapy treatment. *Radiotherapy and Oncology,* 126**,** 339-346.

Dinkel, J., C. Hintze, R. Tetzlaff, P. E. Huber, K. Herfarth, J. Debus, H. U. Kauczor & C. Thieke (2009) 4D-MRI analysis of lung tumor motion in patients with hemidiaphragmatic paralysis. *Radiotherapy and Oncology,* 91**,** 449-454.

Dowling, J., K. Dang, C. D. Fox, S. Chandra, S. Gill, T. Kron, D. Pham & F. Foroudi. 2014. Fast cine-magnetic resonance imaging point tracking for prostate cancer radiation therapy planning. In *Journal of Physics: Conference Series*, 012027. IOP Publishing.

Du, D., S. D. Caruthers, C. Glide-Hurst, D. A. Low, H. H. Li, S. Mutic & Y. Hu (2015) High-quality T2-weighted 4-dimensional magnetic resonance imaging for radiation therapy applications. *International Journal of Radiation Oncology* Biology* Physics,* 92**,** 430-437.

Edmund, J. M. & T. Nyholm (2017) A review of substitute CT generation for MRI-only radiation therapy. *Radiation Oncology,* 12**,** 28.

Ehrbar, S., A. Jöhl, A. Tartas, L. S. Stark, O. Riesterer, S. Klöck, M. Guckenberger & S. Tanadini-Lang (2017) ITV, mid-ventilation, gating or couch tracking–A comparison of respiratory motion-management techniques based on 4D dose calculations. *Radiotherapy and Oncology,* 124**,** 80-88.

Fallone, B. G. 2014. The rotating biplanar linac–magnetic resonance imaging system. In *Seminars in radiation oncology*, 200-202. Elsevier.

Fast, M. F., B. Eiben, M. J. Menten, A. Wetscherek, D. J. Hawkes, J. R. McClelland & U. Oelfke (2017) Tumour auto-contouring on 2d cine MRI for locally advanced lung cancer: A comparative study. *Radiotherapy and Oncology,* 125**,** 485-491.

Fayad, H., H. Schmidt, T. Küstner & D. Visvikis (2017) 4-Dimensional MRI and Attenuation Map Generation in PET/MRI with 4-Dimensional PET-Derived Deformation Matrices: Study of Feasibility for Lung Cancer Applications. *Journal of Nuclear Medicine,* 58**,** 833-839.

Fayad, H. J., C. Buerger, C. Tsoumpas, C. Cheze-Le-Rest & D. Visvikis. 2012. A generic respiratory motion model based on 4D MRI imaging and 2D image navigators. In *Nuclear Science Symposium and Medical Imaging Conference (NSS/MIC), 2012 IEEE*, 4058-4061. IEEE.

Feng, L., L. Axel, H. Chandarana, K. T. Block, D. K. Sodickson & R. Otazo (2016) XD-GRASP: Golden-angle radial MRI with reconstruction of extra motion-state dimensions using compressed sensing. *Magnetic resonance in medicine,* 75**,** 775-788.

Feng, L., R. Grimm, K. T. Block, H. Chandarana, S. Kim, J. Xu, L. Axel, D. K. Sodickson & R. Otazo (2014) Golden-angle radial sparse parallel MRI: Combination of compressed sensing, parallel imaging, and golden-angle radial sampling for fast and flexible dynamic volumetric MRI. *Magnetic resonance in medicine,* 72**,** 707-717.

Feng, M., J. M. Balter, D. Normolle, S. Adusumilli, Y. Cao, T. L. Chenevert & E. Ben-Josef (2009) Characterization of pancreatic tumor motion using cine MRI: surrogates for tumor position should be used with caution. *International Journal of Radiation Oncology* Biology* Physics,* 74**,** 884-891.

Fernandes, A. T., S. Apisarnthanarax, L. Yin, W. Zou, M. Rosen, J. P. Plastaras, E. Ben-Josef, J. M. Metz & B.-K. Teo (2015) Comparative Assessment of Liver Tumor Motion Using Cine–Magnetic Resonance Imaging Versus 4-Dimensional Computed Tomography. *International Journal of Radiation Oncology* Biology* Physics,* 91**,** 1034-1040.

Fontana, G., M. Riboldi, C. Gianoli, C. I. Chirvase, G. Villa, C. Paganelli, P. E. Summers, B. Tagaste, A. Pella & P. Fossati (2016) MRI quantification of pancreas motion as a function of patient setup for particle therapy—a preliminary study. *Journal of Applied Clinical Medical Physics,* 17**,** 60-75.

Ge, J., L. Santanam, C. Noel & P. J. Parikh (2013) Planning 4-dimensional computed tomography (4DCT) cannot adequately represent daily intrafractional motion of abdominal tumors. *International Journal of Radiation Oncology* Biology* Physics,* 85**,** 999-1005.

Glitzner, M., S. Crijns, B. D. De Senneville, C. Kontaxis, F. Prins, J. Lagendijk & B. Raaymakers (2015a) On-line MR imaging for dose validation of abdominal radiotherapy. *Physics in medicine and biology,* 60**,** 8869.

Glitzner, M., S. Crijns, B. D. de Senneville, J. Lagendijk & B. Raaymakers (2015b) On the suitability of Elekta's Agility 160 MLC for tracked radiation delivery: closed-loop machine performance. *Phys Med Biol,* 60**,** 2005-17.

Gou, S., J. Wu, F. Liu, P. Lee, S. Rapacchi, P. Hu & K. Sheng (2014) Feasibility of automated pancreas segmentation based on dynamic MRI. *The British journal of radiology,* 87**,** 20140248.

Griswold, M. A., P. M. Jakob, R. M. Heidemann, M. Nittka, V. Jellus, J. Wang, B. Kiefer & A. Haase (2002) Generalized autocalibrating partially parallel acquisitions (GRAPPA). *Magnetic resonance in medicine,* 47**,** 1202-1210.

Harris, W., L. Ren, J. Cai, Y. Zhang, Z. Chang & F.-F. Yin (2016) A Technique for Generating Volumetric Cine-Magnetic Resonance Imaging. *International Journal of Radiation Oncology* Biology* Physics,* 95**,** 844-853.

Hartman, J., C. Kontaxis, G. Bol, S. Frank, J. Lagendijk, M. van Vulpen & B. Raaymakers (2015) Dosimetric feasibility of intensity modulated proton therapy in a transverse magnetic field of 1.5 T. *Physics in medicine and biology,* 60**,** 5955.

Heerkens, H. D., M. van Vulpen, C. A. van den Berg, R. H. Tijssen, S. P. Crijns, I. Q. Molenaar, H. C. van Santvoort, O. Reerink & G. J. Meijer (2014) MRI-based tumor motion characterization and gating schemes for radiation therapy of pancreatic cancer. *Radiotherapy and Oncology,* 111**,** 252-257.

Heidemann, R. M., Ö. Özsarlak, P. M. Parizel, J. Michiels, B. Kiefer, V. Jellus, M. Müller, F. Breuer, M. Blaimer & M. A. Griswold (2003) A brief review of parallel magnetic resonance imaging. *European radiology,* 13**,** 2323-2337.

Henke, L., R. Kashani, C. Robinson, A. Curcuru, T. DeWees, J. Bradley, O. Green, J. Michalski, S. Mutic & P. Parikh (2018) Phase I trial of stereotactic MR-guided online adaptive radiation therapy (SMART) for the treatment of oligometastatic or unresectable primary malignancies of the abdomen. *Radiotherapy and Oncology,* 126**,** 519-526.

Hoover, D. A., D. P. Capaldi, K. Sheikh, D. A. Palma, G. B. Rodrigues, A. R. Dar, E. Yu, B. Dingle, M. Landis & W. Kocha (2014) Functional lung avoidance for individualized radiotherapy (FLAIR): study protocol for a randomized, double-blind clinical trial. *BMC cancer,* 14**,** 934.

Høyer, M., M. Thor, S. Thörnqvist, J. Søndergaard, Y. Lassen-Ramshad & L. P. Muren (2011) Advances in radiotherapy: from 2D to 4D. *Cancer imaging,* 11**,** S147.

Hu, Y., S. D. Caruthers, D. A. Low, P. J. Parikh & S. Mutic (2013) Respiratory amplitude guided 4-dimensional magnetic resonance imaging. *International Journal of Radiation Oncology* Biology* Physics,* 86**,** 198-204.

Hugo, G. D. & M. Rosu (2012) Advances in 4D radiation therapy for managing respiration: Part I–4D imaging. *Zeitschrift für Medizinische Physik,* 22**,** 258-271.

Hui, C., Z. Wen, B. Stemkens, R. Tijssen, C. Van Den Berg, K.-P. Hwang & S. Beddar (2016) 4D MR imaging using robust internal respiratory signal. *Physics in medicine and biology,* 61**,** 3472.

Hunt, A., V. Hansen, U. Oelfke, S. Nill & S. Hafeez (2018) Adaptive Radiotherapy Enabled by MRI Guidance. *Clinical Oncology*.

ICRU (1999) International Commission on Radiation Units and Measurements: ICRU Report 62. *Prescribing, Recording and Reporting Photon Beam Therapy*.

Jaffray, D. A. (2012) Image-guided radiotherapy: from current concept to future perspectives. *Nature Reviews Clinical Oncology,* 9**,** 688-699.

Jaffray, D. A., M. C. Carlone, M. F. Milosevic, S. L. Breen, T. Stanescu, A. Rink, H. Alasti, A. Simeonov, M. C. Sweitzer & J. D. Winter. 2014. A facility for magnetic resonance–guided radiation therapy. In *Seminars in radiation oncology*, 193-195. Elsevier.

Jiang, N., M. Cao, J. Lamb, K. Sheng, A. Mikaeilian, D. Low, A. Raldow, M. Steinberg & P. Lee (2017a) Outcomes Utilizing MRI-Guided and Real-Time Adaptive Pancreas Stereotactic Body Radiotherapy (SBRT). *International Journal of Radiation Oncology• Biology• Physics,* 99**,** S146.

Jiang, W., F. Ong, K. M. Johnson, S. K. Nagle, T. A. Hope, M. Lustig & P. E. Larson (2017b) Motion robust high resolution 3D free-breathing pulmonary MRI using dynamic 3D image self-navigator. *Magnetic Resonance in Medicine*.

Johnstone, E., J. J. Wyatt, A. M. Henry, S. C. Short, D. Sebag-Montefiore, L. Murray, C. G. Kelly, H. M. McCallum & R. Speight (2017) A systematic review of synthetic CT generation methodologies for use in MRI-only radiotherapy. *International Journal of Radiation Oncology* Biology* Physics,* 100**,** 199-217.

Jonsson, J. H., M. G. Karlsson, M. Karlsson & T. Nyholm (2010) Treatment planning using MRI data: an analysis of the dose calculation accuracy for different treatment regions. *Radiation Oncology,* 5**,** 62.

Karlsson, M., M. G. Karlsson, T. Nyholm, C. Amies & B. Zackrisson (2009) Dedicated magnetic resonance imaging in the radiotherapy clinic. *International Journal of Radiation Oncology* Biology* Physics,* 74**,** 644-651.

Kashani, R. & J. R. Olsen. 2018. Magnetic Resonance Imaging for Target Delineation and Daily Treatment Modification. In *Seminars in Radiation Oncology*, 178-184. Elsevier.

Kauczor, H.-U. & C. Plathow (2006) Imaging tumour motion for radiotherapy planning using MRI. *Cancer Imaging,* 6**,** S140.

Kauczor, H.-U., C. Zechmann, B. Stieltjes & M.-A. Weber (2006) Functional magnetic resonance imaging for defining the biological target volume. *Cancer Imaging,* 6**,** 51-55.

Keall, P. J., M. Barton & S. Crozier. 2014. The Australian magnetic resonance imaging–linac program. In *Seminars in radiation oncology*, 203-206. Elsevier.

Keall, P. J., G. S. Mageras, J. M. Balter, R. S. Emery, K. M. Forster, S. B. Jiang, J. M. Kapatoes, D. A. Low, M. J. Murphy & B. R. Murray (2006) The management of respiratory motion in radiation oncology report of AAPM Task Group 76. *Medical physics,* 33**,** 3874-3900.

Kerkhof, E., J. Balter, K. Vineberg & B. Raaymakers (2010) Treatment plan adaptation for MRI-guided radiotherapy using solely MRI data: a CT-based simulation study. *Physics in medicine and biology,* 55**,** N433.

Keyvanloo, A., B. Burke, B. Warkentin, T. Tadic, S. Rathee, C. Kirkby, D. Santos & B. Fallone (2012) Skin dose in longitudinal and transverse linac-MRIs using Monte Carlo and realistic 3D MRI field models. *Medical physics,* 39**,** 6509-6521.

Kim, T., S. Pollock, D. Lee, R. O'Brien & P. Keall (2012) Audiovisual biofeedback improves diaphragm motion reproducibility in MRI. *Medical physics,* 39**,** 6921-6928.

Kirilova, A., G. Lockwood, P. Choi, N. Bana, M. A. Haider, K. K. Brock, C. Eccles & L. A. Dawson (2008) Three-dimensional motion of liver tumors using cine-magnetic resonance imaging. *International Journal of Radiation Oncology* Biology* Physics,* 71**,** 1189-1195.

Koch, N., H. H. Liu, G. Starkschall, M. Jacobson, K. Forster, Z. Liao, R. Komaki & C. W. Stevens (2004) Evaluation of internal lung motion for respiratory-gated radiotherapy using MRI: Part I—Correlating internal lung motion with skin fiducial motion. *International Journal of Radiation Oncology* Biology* Physics,* 60**,** 1459-1472.

Kontaxis, C., G. Bol, J. Lagendijk & B. Raaymakers (2015a) A new methodology for inter-and intrafraction plan adaptation for the MR-linac. *Physics in medicine and biology,* 60**,** 7485.

--- (2015b) Towards adaptive IMRT sequencing for the MR-linac. *Physics in medicine and biology,* 60**,** 2493.

Kontaxis, C., G. Bol, B. Stemkens, M. Glitzner, F. Prins, L. Kerkmeijer, J. Lagendijk & B. Raaymakers (2017) Towards fast online intrafraction replanning for free-breathing stereotactic body radiation therapy with the MR-linac. *Physics in Medicine & Biology,* 62**,** 7233.

Korreman, S. S. (2012) Motion in radiotherapy: photon therapy. *Physics in medicine and biology,* 57**,** R161.

Krauss, A., S. Nill & U. Oelfke (2011) The comparative performance of four respiratory motion predictors for real-time tumour tracking. *Physics in medicine and biology,* 56**,** 5303.

Kubiak, T. (2016) Particle therapy of moving targets—the strategies for tumour motion monitoring and moving targets irradiation. *The British journal of radiology,* 89**,** 20150275.

Kurz, C., G. Landry, A. F. Resch, G. Dedes, F. Kamp, U. Ganswindt, C. Belka, B. W. Raaymakers & K. Parodi (2017) A Monte-Carlo study to assess the effect of 1.5 T magnetic fields on the overall robustness of pencil-beam scanning proton radiotherapy plans for prostate cancer. *Physics in Medicine & Biology,* 62**,** 8470.

Küstner, T., C. Würslin, M. Schwartz, P. Martirosian, S. Gatidis, C. Brendle, F. Seith, F. Schick, N. F. Schwenzer & B. Yang (2017) Self-navigated 4D cartesian imaging of periodic motion in the body trunk using partial k-space compressed sensing. *Magnetic resonance in medicine,* 78**,** 632-644.

Lagendijk, J. J., B. W. Raaymakers, C. A. Van den Berg, M. A. Moerland, M. E. Philippens & M. Van Vulpen (2014) MR guidance in radiotherapy. *Physics in medicine and biology,* 59**,** R349.

Lee, D., P. B. Greer, J. Ludbrook, J. Arm, P. Hunter, S. Pollock, K. Makhija, R. T. O'brien, T. Kim & P. Keall (2016) Audiovisual Biofeedback Improves Cine–Magnetic Resonance Imaging Measured Lung Tumor Motion Consistency. *International Journal of Radiation Oncology* Biology* Physics,* 94**,** 628-636.

Lens, E., A. van der Horst, E. Versteijne, G. van Tienhoven & A. Bel (2015) Dosimetric advantages of midventilation compared with internal target volume for radiation therapy of pancreatic cancer. *International Journal of Radiation Oncology* Biology* Physics,* 92**,** 675-682.

Li, G., J. Wei, D. Olek, M. Kadbi, N. Tyagi, K. Zakian, J. Mechalakos, J. O. Deasy & M. Hunt (2016) Direct Comparison of Respiration-Correlated Four-Dimensional Magnetic Resonance Imaging Reconstructed Using Concurrent Internal Navigator and External Bellows. *International Journal of Radiation Oncology* Biology* Physics*.

--- (2017) Direct comparison of respiration-correlated four-dimensional magnetic resonance imaging reconstructed using concurrent internal navigator and external bellows. *International Journal of Radiation Oncology* Biology* Physics,* 97**,** 596-605.

Li, J. G. & L. Xing (2000) Inverse planning incorporating organ motion. *Medical physics,* 27**,** 1573-1578.

Liang, X., F. F. Yin, Y. Liu & J. Cai (2016) A probability-based multi-cycle sorting method for 4D-MRI: A simulation study. *Medical Physics,* 43**,** 6375-6385.

Liu, H. H., N. Koch, G. Starkschall, M. Jacobson, K. Forster, Z. Liao, R. Komaki & C. W. Stevens (2004) Evaluation of internal lung motion for respiratory-gated radiotherapy using MRI: Part II—Margin reduction of internal target volume. *International Journal of Radiation Oncology* Biology* Physics,* 60**,** 1473-1483.

Liu, Y., F.-F. Yin, B. G. Czito, M. R. Bashir, M. Palta & J. Cai (2017) Retrospective four-dimensional magnetic resonance imaging with image-based respiratory surrogate: a sagittal–coronal–diaphragm point of intersection motion tracking method. *Journal of Medical Imaging,* 4**,** 024007.

Liu, Y., F. F. Yin, Z. Chang, B. G. Czito, M. Palta, M. R. Bashir, Y. Qin & J. Cai (2014a) Investigation of sagittal image acquisition for 4D-MRI with body area as respiratory surrogate. *Medical physics,* 41**,** 101902.

--- (2014b) Investigation of sagittal image acquisition for 4D-MRI with body area as respiratory surrogate. *Medical physics,* 41.

Liu, Y., F. F. Yin, B. G. Czito, M. R. Bashir & J. Cai (2015) T2-weighted four dimensional magnetic resonance imaging with result-driven phase sorting. *Medical physics,* 42**,** 4460-4471.

Liu, Y., F. F. Yin, D. Rhee & J. Cai (2016a) Accuracy of respiratory motion measurement of 4D-MRI: A comparison between cine and sequential acquisition. *Medical physics,* 43**,** 179-187.

Liu, Y., X. Zhong, B. G. Czito, M. Palta, M. R. Bashir, B. M. Dale, F. F. Yin & J. Cai (2016b) Four-Dimensional Diffusion-Weighted MR imaging (4D-DWI): A Feasibility Study. *Medical Physics,* 44**,** 397-406.

Lustig, M., D. L. Donoho, J. M. Santos & J. M. Pauly (2008) Compressed sensing MRI. *IEEE signal processing magazine,* 25**,** 72-82.

Marx, M., J. Ehrhardt, R. Werner, H.-P. Schlemmer & H. Handels (2014) Simulation of spatiotemporal CT data sets using a 4D MRI-based lung motion model. *International journal of computer assisted radiology and surgery,* 9**,** 401-409.

Maspero, M., C. A. Van den Berg, G. Landry, C. Belka, K. Parodi, P. R. Seevinck, B. W. Raaymakers & C. Kurz (2017) Feasibility of MR-only proton dose calculations for prostate cancer radiotherapy using a commercial pseudo-CT generation method. *Physics in Medicine & Biology,* 62**,** 9159.

Mazur, T. R., B. W. Fischer-Valuck, Y. Wang, D. Yang, S. Mutic & H. H. Li (2016) SIFT-based dense pixel tracking on 0.35 T cine-MR images acquired during image-guided radiation therapy with application to gating optimization. *Medical physics,* 43**,** 279-293.

McClelland, J. R., D. J. Hawkes, T. Schaeffter & A. P. King (2013) Respiratory motion models: A review. *Medical image analysis,* 17**,** 19-42.

McClelland, J. R., M. Modat, S. Arridge, H. Grimes, D. D'Souza, D. Thomas, D. O. Connell, D. A. Low, E. Kaza, D. J. Collins, M. O. Leach & D. J. Hawkes (2017) A generalized framework unifying image registration and respiratory motion models and incorporating image reconstruction, for partial image data or full images. *Physics in Medicine & Biology,* 62**,** 4273-4292.

McRobbie, D. W., E. A. Moore & M. J. Graves. 2017. *MRI from Picture to Proton*. Cambridge university press.

Ménard, C. & U. van der Heide. 2014. Introduction: Systems for magnetic resonance image guided radiation therapy. In *Seminars in radiation oncology*, 192. Elsevier.

Menten, M. J., A. Wetscherek & M. F. Fast (2017) MRI-guided lung SBRT: Present and future developments. *Physica Medica,* 139**,** 139-149.

Mickevicius, N. J. & E. S. Paulson (2017a) Investigation of undersampling and reconstruction algorithm dependence on respiratory correlated 4D-MRI for online MR-guided radiation therapy. *Physics in medicine and biology,* 62**,** 2910.

--- (2017b) Simultaneous orthogonal plane imaging. *Magnetic resonance in medicine,* 78**,** 1700-1710.

Mutic, S. & J. F. Dempsey. 2014. The ViewRay system: Magnetic resonance–guided and controlled radiotherapy. In *Seminars in radiation oncology*, 196-199. Elsevier.

Oborn, B., S. Kolling, P. E. Metcalfe, S. Crozier, D. Litzenberg & P. Keall (2014) Electron contamination modeling and reduction in a 1 T open bore inline MRI-linac system. *Medical physics,* 41.

Oborn, B. M., S. Dowdell, P. E. Metcalfe, S. Crozier, R. Mohan & P. J. Keall (2017) Future of Medical Physics: Real-time MRI guided Proton Therapy. *Medical Physics,* 44**,** e77-e90.

Oborn, B. M., Y. Ge, N. Hardcastle, P. E. Metcalfe & P. J. Keall (2016) Dose enhancement in radiotherapy of small lung tumors using inline magnetic fields: A Monte Carlo based planning study. *Medical physics,* 43**,** 368-377.

Odille, F., P.-A. Vuissoz, P.-Y. Marie & J. Felblinger (2008) Generalized Reconstruction by Inversion of Coupled Systems (GRICS) applied to free-breathing MRI. *Magnetic Resonance in Medicine,* 60**,** 146-157.

Olsen, J., O. Green & R. Kashani (2014) World's First Application of MR-Guidance for Radiotherapy. *Missouri medicine,* 112**,** 358-360.

Paganelli, C., J. Kipritidis, D. Lee, G. Baroni, P. Keall & M. Riboldi (2018) Image-based retrospective 4D MRI in external beam radiotherapy: A comparative study with a digital phantom. *Med Phys.*

Paganelli, C., D. Lee, P. B. Greer, G. Baroni, M. Riboldi & P. Keall (2015a) Quantification of lung tumor rotation with automated landmark extraction using orthogonal cine MRI images. *Physics in medicine and biology,* 60**,** 7165.

Paganelli, C., M. Seregni, G. Fattori, P. Summers, M. Bellomi, G. Baroni & M. Riboldi (2015b) Magnetic resonance imaging–guided versus surrogate-based motion tracking in liver radiation therapy: A prospective comparative study. *International Journal of Radiation Oncology* Biology* Physics,* 91**,** 840-848.

Paganelli, C., P. Summers, M. Bellomi, G. Baroni & M. Riboldi (2015c) Liver 4DMRI: A retrospective image-based sorting method. *Medical physics,* 42**,** 4814-4821.

Park, S., R. Farah, S. M. Shea, E. Tryggestad, R. Hales & J. Lee (2018) Simultaneous tumor and surrogate motion tracking with dynamic MRI for radiation therapy planning. *Physics in Medicine & Biology,* 63**,** 025015.

Plathow, C., M. Klopp, C. Fink, A. Sandner, H. Hof, M. Puderbach, F. Herth, A. Schmähl & H. Kauczor (2005) Quantitative analysis of lung and tumour mobility: comparison of two time-resolved MRI sequences. *The British journal of radiology*.

Plathow, C., S. Ley, C. Fink, M. Puderbach, W. Hosch, A. Schmähl, J. Debus & H.-U. Kauczor (2004) Analysis of intrathoracic tumor mobility during whole breathing cycle by dynamic MRI. *International Journal of Radiation Oncology* Biology* Physics,* 59**,** 952-959.

Plathow, C., M. Schoebinger, C. Fink, H. Hof, J. r. Debus, H.-P. Meinzer & H.-U. Kauczor (2006) Quantification of Lung Tumor Volume and Rotation at 3D Dynamic Parallel MR Imaging with View Sharing: Preliminary Results 1. *Radiology,* 240**,** 537-545.

Plathow, C., M. Schoebinger, F. Herth, S. Tuengerthal, H.-P. Meinzer & H.-U. Kauczor (2009) Estimation of pulmonary motion in healthy subjects and patients with intrathoracic tumors using 3D-dynamic MRI: initial results. *Korean journal of radiology,* 10**,** 559-567.

Prestwich, R., S. Vaidyanathan & A. Scarsbrook (2015) Functional imaging biomarkers: potential to guide an individualised approach to radiotherapy. *Clinical Oncology,* 27**,** 588-600.

Pruessmann, K. P. (2006) Encoding and reconstruction in parallel MRI. *NMR in Biomedicine,* 19**,** 288-299.

Raaijmakers, A., B. Hårdemark, B. Raaymakers, C. Raaijmakers & J. Lagendijk (2007) Dose optimization for the MRI-accelerator: IMRT in the presence of a magnetic field. *Physics in medicine and biology,* 52**,** 7045.

Raaymakers, B., I. Jürgenliemk-Schulz, G. Bol, M. Glitzner, A. Kotte, B. van Asselen, J. de Boer, J. Bluemink, S. Hackett & M. Moerland (2017) First patients treated with a 1.5 T MRI-Linac: clinical proof of concept of a high-precision, high-field MRI guided radiotherapy treatment. *Physics in Medicine & Biology,* 62**,** L41.

Rank, C. M., T. Heußer, M. T. Buzan, A. Wetscherek, M. T. Freitag, J. Dinkel & M. Kachelrieß (2017) 4D respiratory motion-compensated image reconstruction of free-breathing radial MR data with very high undersampling. *Magnetic resonance in medicine,* 77**,** 1170-1183.

Rank, C. M., T. Heußer, A. Wetscherek, M. T. Freitag, O. Sedlaczek, H. P. Schlemmer & M. Kachelrieß (2016) Respiratory motion compensation for simultaneous PET/MR based on highly undersampled MR data. *Medical physics,* 43**,** 6234-6245.

Riboldi, M., R. Orecchia & G. Baroni (2012) Real-time tumour tracking in particle therapy: technological developments and future perspectives. *The lancet oncology,* 13**,** e383-e391.

Rohlfing, T., C. R. Maurer, W. G. O'Dell & J. Zhong (2004) Modeling liver motion and deformation during the respiratory cycle using intensity-based nonrigid registration of gated MR images. *Medical Physics,* 31**,** 427-432.

Rosenblatt, E. & E. Zubizarreta (2017) RADIOTHERAPY IN CANCER CARE: FACING THE GLOBAL CHALLENGE. *International Atomic Energy Agency*.

Rosu, M. & G. D. Hugo (2012) Advances in 4D radiation therapy for managing respiration: part II–4D treatment planning. *Zeitschrift für Medizinische Physik,* 22**,** 272-280.

Ruan, D., J. A. Fessler, J. Balter, R. Berbeco, S. Nishioka & H. Shirato (2008) Inference of hysteretic respiratory tumor motion from external surrogates: a state augmentation approach. *Physics in Medicine & Biology,* 53**,** 2923.

Ruschin, M., A. Sahgal, C.-L. Tseng, M. Sonier, B. Keller & Y. Lee (2017) Dosimetric Impact of Using a Virtual Couch Shift for Online Correction of Setup Errors for Brain Patients on an Integrated High-Field Magnetic Resonance Imaging Linear Accelerator. *International Journal of Radiation Oncology* Biology* Physics,* 98**,** 699-708.

Sawant, A., P. Keall, K. B. Pauly, M. Alley, S. Vasanawala, B. W. Loo Jr, J. Hinkle & S. Joshi (2014a) Investigating the feasibility of rapid MRI for image-guided motion management in lung cancer radiotherapy. *BioMed research international,* 2014.

--- (2014b) Investigating the feasibility of rapid MRI for image-guided motion management in lung cancer radiotherapy. *BioMed research international,* 2014**,** 485067.

Schmidt, M. A. & G. S. Payne (2015) Radiotherapy planning using MRI. *Physics in medicine and biology,* 60**,** R323.

Schwarz, M., G. M. Cattaneo & L. Marrazzo (2017) Geometrical and dosimetrical uncertainties in hypofractionated radiotherapy of the lung: A review. *Physica Medica*.

Seregni, M., C. Paganelli, D. Lee, P. Greer, G. Baroni, P. Keall & M. Riboldi (2016) Motion prediction in MRI-guided radiotherapy based on interleaved orthogonal cine-MRI. *Physics in medicine and biology,* 61**,** 872.

Seregni, M., C. Paganelli, P. Summers, M. Bellomi, G. Baroni & M. Riboldi (2017) A hybrid image registration and matching framework for real-time motion tracking in MRI-guided radiotherapy. *IEEE Transactions on Biomedical Engineering,* 65**,** 131-139.

Shi, X., T. Diwanji, K. E. Mooney, J. Lin, S. Feigenberg, W. D. D'Souza & N. N. Mistry (2014) Evaluation of template matching for tumor motion management with cine-MR images in lung cancer patients. *Medical physics,* 41.

Simpson, D. R., J. D. Lawson, S. K. Nath, B. S. Rose, A. J. Mundt & L. K. Mell (2009) Utilization of advanced imaging technologies for target delineation in radiation oncology. *Journal of the American College of Radiology,* 6**,** 876-883.

Song, R., A. Tipirneni, P. Johnson, R. B. Loeffler & C. M. Hillenbrand (2011) Evaluation of respiratory liver and kidney movements for MRI navigator gating. *Journal of Magnetic Resonance Imaging,* 33**,** 143-148.

Stam, M. K., M. Van Vulpen, M. M. Barendrecht, B. A. Zonnenberg, S. P. Crijns, J. J. Lagendijk & B. W. Raaymakers (2013a) Dosimetric feasibility of MRI-guided external beam radiotherapy of the kidney. *Physics in medicine and biology,* 58**,** 4933.

Stam, M. K., M. Van Vulpen, M. M. Barendrecht, B. A. Zonnenberg, M. Intven, S. P. Crijns, J. J. Lagendijk & B. W. Raaymakers (2013b) Kidney motion during free breathing and breath hold for MR-guided radiotherapy. *Physics in medicine and biology,* 58**,** 2235.

Stemkens, B., M. Glitzner, C. Kontaxis, B. D. De Senneville, F. M. Prins, S. P. Crijns, L. G. Kerkmeijer, J. J. Lagendijk, C. A. Van Den Berg & R. H. Tijssen (2017) Effect of intra-fraction motion on the accumulated dose for free-breathing MR-guided stereotactic body radiation therapy of renal-cell carcinoma. *Physics in Medicine & Biology,* 62**,** 7407.

Stemkens, B., R. H. Tijssen, B. D. de Senneville, H. D. Heerkens, M. van Vulpen, J. J. Lagendijk & C. A. van den Berg (2015) Optimizing 4-dimensional magnetic resonance imaging data sampling for respiratory motion analysis of pancreatic tumors. *International Journal of Radiation Oncology* Biology* Physics,* 91**,** 571-578.

Stemkens, B., R. H. Tijssen, B. D. de Senneville, J. J. Lagendijk & C. A. van den Berg (2016) Image-driven, model-based 3D abdominal motion estimation for MR-guided radiotherapy. *Physics in Medicine and Biology,* 61**,** 5335.

Thomas, D. H., A. Santhanam, A. U. Kishan, M. Cao, J. Lamb, Y. Min, D. O'Connell, Y. Yang, N. Agazaryan & P. Lee (2017) Initial observations of intra-and inter-fractional motion variation in MR guided lung SBRT. *The British Journal of Radiology***,** 20170522.

To, D. T., J. P. Kim, R. G. Price, I. J. Chetty & C. K. Glide-Hurst (2016a) Impact of incorporating visual biofeedback in 4D MRI. *Journal of Applied Clinical Medical Physics,* 17.

--- (2016b) Impact of incorporating visual biofeedback in 4D MRI. *Journal of Applied Clinical Medical Physics,* 17**,** 128-137.

Tokuda, J., S. Morikawa, H. A. Haque, T. Tsukamoto, K. Matsumiya, H. Liao, K. Masamune & T. Dohi (2008) Adaptive 4D MR imaging using navigator-based respiratory signal for MRI-guided therapy. *Magnetic resonance in medicine,* 59**,** 1051-1061.

Torfeh, T., R. Hammoud, T. El Kaissi, M. McGarry, S. Aouadi, H. Fayad & N. Al-Hammadi (2018) Geometric accuracy of the MR imaging techniques in the presence of motion. *Journal of applied clinical medical physics,* 19**,** 168-175.

Tryggestad, E., A. Flammang, R. Hales, J. Herman, J. Lee, T. McNutt, T. Roland, S. M. Shea & J. Wong (2013a) 4D tumor centroid tracking using orthogonal 2D dynamic MRI: Implications for radiotherapy planning. *Medical physics,* 40.

--- (2013b) 4D tumor centroid tracking using orthogonal 2D dynamic MRI: Implications for radiotherapy planning. *Medical physics,* 40**,** 091712.

Tryggestad, E., A. Flammang, S. Han-Oh, R. Hales, J. Herman, T. McNutt, T. Roland, S. M. Shea & J. Wong (2013c) Respiration-based sorting of dynamic MRI to derive representative 4D-MRI for radiotherapy planning. *Medical physics,* 40.

--- (2013d) Respiration-based sorting of dynamic MRI to derive representative 4D-MRI for radiotherapy planning. *Medical physics,* 40**,** 051909.

Uh, J., M. A. Khan & C. Hua (2016) Four-dimensional MRI using an internal respiratory surrogate derived by dimensionality reduction. *Physics in Medicine and Biology,* 61**,** 7812.

Unkelbach, J. & U. Oelfke (2004) Inclusion of organ movements in IMRT treatment planning via inverse planning based on probability distributions. *Physics in medicine and biology,* 49**,** 4005.

van de Lindt, T., J.-J. Sonke, M. Nowee, E. Jansen, V. van Pelt, U. van der Heide & M. Fast (2018a) A self-sorting coronal 4D-MRI method for daily image guidance of liver lesions on an MR-Linac. *International Journal of Radiation Oncology• Biology• Physics*.

van de Lindt, T. N., M. F. Fast, U. A. van der Heide & J.-J. Sonke (2018b) Retrospective self-sorted 4D-MRI for the liver. *Radiotherapy and Oncology*.

van de Lindt, T. N., G. Schubert, U. A. van der Heide & J.-J. Sonke (2016) An MRI-based mid-ventilation approach for radiotherapy of the liver. *Radiotherapy and Oncology,* 121**,** 276-280.

van der Heide, U. A., A. C. Houweling, G. Groenendaal, R. G. Beets-Tan & P. Lambin (2012) Functional MRI for radiotherapy dose painting. *Magnetic resonance imaging,* 30**,** 1216-1223.

Van Heijst, T. C., M. E. Philippens, R. K. Charaghvandi, M. D. Den Hartogh, J. J. Lagendijk, H. D. van den Bongard & B. van Asselen (2016) Quantification of intra-fraction motion in breast radiotherapy using supine magnetic resonance imaging. *Physics in medicine and biology,* 61**,** 1352.

Van Herk, M. 2004. Errors and margins in radiotherapy. In *Seminars in radiation oncology*, 52-64. Elsevier.

Varoquaux, A., O. Rager, P. Dulguerov, K. Burkhardt, A. Ailianou & M. Becker (2015) Diffusion-weighted and PET/MR imaging after radiation therapy for malignant head and neck tumors. *Radiographics,* 35**,** 1502-1527.

Venselaar, J., H. Welleweerd & B. Mijnheer (2001) Tolerances for the accuracy of photon beam dose calculations of treatment planning systems. *Radiotherapy and oncology,* 60**,** 191-201.

Verellen, D., M. De Ridder & G. Storme (2008) A (short) history of image-guided radiotherapy. *Radiotherapy and Oncology,* 86**,** 4-13.

Von Siebenthal, M., G. Székely, U. Gamper, P. Boesiger, A. Lomax & P. Cattin (2007) 4D MR imaging of respiratory organ motion and its variability. *Physics in medicine and biology,* 52**,** 1547.

Wachinger, C., M. Yigitsoy, E.-J. Rijkhorst & N. Navab (2012) Manifold learning for image-based breathing gating in ultrasound and MRI. *Medical image analysis,* 16**,** 806-818.

Weick, S., M. Völker, K. Hemberger, C. Meyer, P. Ehses, B. Polat, F. A. Breuer, M. Blaimer, C. Fink & L. R. Schad (2017) Desynchronization of Cartesian k-space sampling and periodic motion for improved retrospectively self-gated 3D lung MRI using quasi-random numbers. *Magnetic resonance in medicine,* 77**,** 787-793.

Weiss, J., M. Notohamiprodjo, P. Martirosian, J. Taron, M. D. Nickel, M. Kolb, F. Bamberg, K. Nikolaou & A. E. Othman (2017) Self-gated 4D-MRI of the liver: Initial clinical results of continuous multiphase imaging of hepatic enhancement. *Journal of Magnetic Resonance Imaging*.

Whelan, B., G. P. Liney, J. A. Dowling, R. Rai, L. Holloway, L. McGarvie, I. Feain, M. Barton, M. Berry & R. Wilkins (2017) An MRI-compatible patient rotation system—design, construction, and first organ deformation results. *Medical physics,* 44**,** 581-588.

Wojcieszynski, A. P., S. A. Rosenberg, J. V. Brower, C. R. Hullett, M. W. Geurts, Z. E. Labby, P. M. Hill, R. A. Bayliss, B. Paliwal & J. E. Bayouth (2016) Gadoxetate for direct tumor therapy and tracking with real-time MRI-guided stereotactic body radiation therapy of the liver. *Radiotherapy and Oncology,* 118**,** 416-418.

Wolthaus, J. W., C. Schneider, J.-J. Sonke, M. van Herk, J. S. Belderbos, M. M. Rossi, J. V. Lebesque & E. M. Damen (2006) Mid-ventilation CT scan construction from four-dimensional respiration-correlated CT scans for radiotherapy planning of lung cancer patients. *International Journal of Radiation Oncology* Biology* Physics,* 65**,** 1560-1571.

Wolthaus, J. W., J.-J. Sonke, M. van Herk, J. S. Belderbos, M. M. Rossi, J. V. Lebesque & E. M. Damen (2008) Comparison of different strategies to use four-dimensional computed tomography in treatment planning for lung cancer patients. *International Journal of Radiation Oncology* Biology* Physics,* 70**,** 1229-1238.

Yang, Y., M. Cao, K. Sheng, Y. Gao, A. Chen, M. Kamrava, P. Lee, N. Agazaryan, J. Lamb & D. Thomas (2016) Longitudinal diffusion MRI for treatment response assessment: Preliminary experience using an MRI-guided tri-cobalt 60 radiotherapy system. *Medical physics,* 43**,** 1369-1373.

Yun, J., M. Mackenzie, S. Rathee, D. Robinson & B. Fallone (2012) An artificial neural network (ANN)-based lung-tumor motion predictor for intrafractional MR tumor tracking. *Medical physics,* 39**,** 4423-4433.

Yun, J., E. Yip, Z. Gabos, K. Wachowicz, S. Rathee & B. G. Fallone (2015) Neural-network based autocontouring algorithm for intrafractional lung-tumor tracking using Linac-MR. *Medical Physics,* 42**,** 2296-2310.

Zachiu, C., N. Papadakis, M. Ries, C. Moonen & B. D. de Senneville (2015) An improved optical flow tracking technique for real-time MR-guided beam therapies in moving organs. *Physics in medicine and biology,* 60**,** 9003.

Zhang, Y., I. Huth, M. Wegner, D. C. Weber & A. J. Lomax (2016) An evaluation of rescanning technique for liver tumour treatments using a commercial PBS proton therapy system. *Radiotherapy and oncology,* 121**,** 281-287.

Zhang, Y., A. Knopf, C. Tanner & A. Lomax (2014) Online image guided tumour tracking with scanned proton beams: a comprehensive simulation study. *Physics in medicine and biology,* 59**,** 7793.

Zucker, E. J., J. Y. Cheng, A. Haldipur, M. Carl & S. S. Vasanawala (2017) Free-breathing pediatric chest MRI: Performance of self-navigated golden-angle ordered conical ultrashort echo time acquisition. *Journal of Magnetic Resonance Imaging,* 47**,** 200-209.